2024 | JANUARY - DECEMBER 6th YEAR 1st EDITION

IJIET

INTERNATIONAL JOURNAL OF INDUSTRIAL EDUCATION AND TECHNOLOGY

SCHOOL OF INDUSTRIAL EDUCATION AND TECHNOLOGY
KING MONGKUT'S INSTITUTE OF TECHNOLOGY LADKRABANG

International Journal of Industrial Education and Technology
ISSN 2673-0448
Vol. 6 No. 1 (January–December) 2024

International Journal of Industrial Education and Technology Editor Board

Assoc. Prof. Dr. Tuanjai Archevapanich	Rajamangala University of Technology Suvarnabhumi, Nonthaburi
Assoc. Prof. Dr. Udomvit Chaisakulkiet	Rajamangala University of Technology Rattanakosin
Assoc. Prof. Attarporn Ridhikerd	(Retired civil servant)
	Anusawari sub-district, Bang Khen district, Bangkok
Asst. Prof. Dr. Anusit Anmanatarkul	King Mongkut's University of Technology Thonburi
Asst. Prof. Dr. Janpanit Surasin	Burapha University
Asst. Prof. Dr. Pattama Pattanapong	Mahidol University
Asst. Prof. Dr. Petcharat Suriyachai	Prince of Songkla University
Asst. Prof. Dr. Sasitorn Suwannathep	King Mongkut's University of Technology Thonburi
Asst. Prof. Dr. Suchada Katdee	Rajamangala University of Technology Phra Nakhon
Asst. Prof. Dr. Suebpong Prabyai	Ramkhamhaeng University
Asst. Prof. Dr. Thosporn Sangsawang	Rajamangala University of Technology Thanyaburi
Asst. Prof. Dr. Yupin Phasuk	Khon Kaen University
Asst. Prof. Pramote Anunvarapong	Rajamangala University of Technology Krungthep
Dr. Bundit Prasantree	Phranakhon Rajabhat University
Dr. Kiattisak Siphimanwat	National Electronics and Computer Technology Center
Dr. Pakorn Prajuabwan	Kanchanaburi Rajabhat University
Dr. Saowalak Saengkae	Rajamangala University of Technology Krungthep
Dr. Somjai Klin-Ngam	Phranakhon Rajabhat University University
Dr. Somporn Seewattanapon	Rajamangala University of Technology Suvarnabhumi

2.3 Internal Editor Board Committees (King Mongkut's Institute of Technology Ladkrabang)

Prof. Dr. Pakkapong Poungsuk,
Asst.Prof. Dr. Somchai Seviset
Asst.Prof. Dr. Somchai Maunsaiyat
Asst.Prof. Dr. Apirath Limmanee
Assoc.Prof. Dr. Pornpimon Chayratsami
Dr. Thadharphut Limapornvanitr

3. Design and Approved Printing

(Thai Language Approval)

Asst. Prof. Dr. Ampapan Tuntinakhongul
Asst. Prof. Dr. Jatuporn Anuchai

(English Language Approval)

Asst. Prof. Dr. Ampapan Tuntinakhongul

Cover Design

Mr.Teeraphat Naegkhunthod

Information Technology

Assoc. Prof. Dr. Piya Supavarasuwat

Mr.Mai Charoentham

Mr.Prayoot Kunthong

Mrs.Jantanee Supsaendee

4. Membership Service

Mrs.Jantanee Supsaendee

5. Registration Service

Mrs.Jantanee Supsaendee

6. Assistant Editor

Mrs.Jantanee Supsaendee

Publishing: One issue per year

The 1st issue for January to December

Submission: Continuously

Scopes

Publication on academic and research articles in the terms of **Industrial Education** and **Education and Technology** in specific fields as

1. Teaching/Education
2. Engineering
3. Architecture
4. Agriculture

Selecting speculator for article criteria

Criteria from speculators as follows:

- Article from individual inside institute is speculated by only speculators outside institute.
- Article from individual outside institute is speculated by one speculator inside institute and two speculators outside institute.

Website: https://www.tci-thaijo.org/index.php/IJIET

E-mail: journal-enided@kmitl.ac.th

Address: School of Industrial Education and Technology,
King Mongkut's Institute of Technology Ladkrabang
No.1, Soi Chalongkrung 1, Chalongkrung Road,
Ladkrabang, Bangkok, 10520
Tel: 08 6349 6020 or 02 329 8000 ext.3723
Fax: 02 329 8435

Editorial Statement

As an editor in chief of International Journal of Industrial Education and Technology (IJIET), I would like to welcome and present you the 2024 issue which is mainly to offer the research contents and articles in the fields of industrial education including education and technology. IJIET is consisted by three contents which are review article, book review, and research articles, respectively. For this IJIET issue, review article is on "COMPARATIVE STUDY OF SELF-IMPOSED DOUBLE ROLES IN ONLINE STREAMING OF SOCIAL DEDUCTION GAMES" and book review is about "DESIGNING EFFECTIVE INSTRUCTION (7TH EDITION), 2013 GARY R. MORRISON, STEVEN M. ROSS, HOWARD K. KALMAN, AND JERALD E. KEMP". Research articles are focused on researches in creative economic creation and technology, ionospheric and space weather study, and satellite technology. I would like to invite you to read all interesting contents authored by the professional and intelligent group of writers who are volunteers to share their outcomes of research and professional discussions.

On behalf of the editorial boards, I would like to sincerely delight to thank you very much for your kindly support. If you would like to make us the comments and give us the suggestions regarding on this issue, I would be appreciated and sincerely accepted that to make things better.

With best regards,

Associate Professor Dr. Prasert Kenpankho, D.Eng.
Editor in Chief
International Journal of Industrial Education and Technology (IJIET)

Contents	Page

IJIET
INTERNATIONAL JOURNAL
OF INDUSTRIAL EDUCATION AND TECHNOLOGY
ISSN 2673-0448

Review Article

COMPARATIVE STUDY OF SELF-IMPOSED DOUBLE ROLES IN ONLINE STREAMING OF SOCIAL DEDUCTION GAMES

Apirath Limmanee*
Email: apirath.li@kmitl.ac.th*

Received: April 26, 2024
Revised: June 21, 2024
Accepted: July 19, 2024

ABSTRACT

For game streamers, the main objective in playing social deduction games is not only to win the games but also to make the gameplay more dramatic and enjoyable so that larger audience can be attracted. Streamers of social deduction games usually employ storytelling and comedy techniques to emphasize the surreal, dramatic, and mysterious aspects of their games. However, there are limitations given by the roles obtained in each gameplay. Some roles (for example, impostor) are more dramatic than others (for example, crewmate). Therefore, while being given a particular role, some steamers desire other roles that they can better express themselves.

In this paper, we will use the term “Double roles” to describe this phenomenon resulting from players’ longings for more exalted roles than given ones. The act of assuming double roles usually occurs after some important information regarding the enemy identity is revealed to them, allowing them to make some forms of “contracts” with the pre-assigned enemies.

Keywords: Social deduction games, Online games, Video games, Streaming, Psychology, Double roles

*Corresponding Author E-mail: apirath.li@kmitl.ac.th
[1*]Department of Enginering Education, School of Industrial Education and Technology,
King Mongkut’s Institute of Technology Ladkrabang, Bangkok 10520 Thailand

I. PROBLEMS IN STRATEGIC APPROACH TO SOCIAL DEDUCTION GAMES AND INTRODUCTION TO SITUATIONAL COMPARATIVE APPROACH

In the research literature of the present time, the time that sees the progressive development and popularity of online video games, there are papers trying to penetrate beyond the surface of joy and laughter in social deduction games, in order to portray and interpret the subtle player strategies. (Eger & Martens, 2018, pp. 24-30; Kopparapu et al., 2022, pp. 1-11; Wiseman & Lewis, 2019, pp. 781-787).

Strategies of a "good guy" in a social deduction game generally aim at uncovering other players' roles and additional secret information, occasionally from manifest evidence. Also, good players playing as good guys do not shy away from seemingly random observations, investigations, or inquiries, in the game, because those playing as bad guys will try to make any possible evidence as obscure as possible.

One of the challenges faced by the players of social deduction games when playing the games is the lack of concepts to describe and predict the behaviors of other players. For example, in the game "Among Us," although we know that players gathering in a dense group at a specific game map's location will likely lead to murders as it is difficult to see who kill who, we do not know when murders will occur and who will kill or be killed.

Even when strategic approach is taken, we cannot say that one strategy matters only for the "bad guy" roles, while another applies only to "good guys." What really matters is the fundamental framework combining several strategies. For the framework to be fundamental as assumed, it must be able to explain the playing behavior of all parties from the start to the end of the game. In addition, it must be able to explain chronological development of each character as well as to reveal essential relationships among characters.

In the bigger picture, it is very difficult, if not impossible, to predict the impact of introducing new maps in the same game, new variations of social deduction games, or new roles in the same game. Social deduction games evolve dynamically over time, providing different sets of rules, complex interactions among players, tasks, side quests, as well as other elements in game environment (Rank, 1989).

Therefore, there should be no objection if we take, as the point of departure, the dramatic scenes in the game, which lead to insightful joy and laughter as well as contribute to its popularity. After that, in future work, we can thus trace back the history of traditional social deduction games such as Werewolf (Mafia) which has stimulated subsequent imaginative and thoughtful game designers.

Our task can only become comprehensive and generalized by considering the significant differences in game environments and rules from which playing styles and strategies are originated. This comparative method seeks not so much to establish similarities as to form an extension of meaning concatenated from the earliest social deduction games played in a party to today's games played online.

II. DOUBLE ROLES IN ONLINE STREAMING OF SOCIAL DEDUCTION GAMES

For game streamers, the main objective in playing social deduction games is not only to win the games but also to make the gameplay more dramatic and enjoyable so that larger audience can be attracted. Streamers of social deduction games usually employ storytelling and comedy techniques to emphasize the surreal, dramatic, and mysterious aspects of their games. However, there are limitations given by the roles obtained in each gameplay. Some roles (for example, impostor) are more dramatic than others (for example, crewmate). Therefore, while being given a particular role, some steamers desire other roles that they can better express themselves.

In this paper, we will use the term “double roles” to describe this phenomenon resulting from players’ longings for more exalted roles than given ones. It should be noted that this more frequently happens when the given roles are, by nature, unsure about others’. It is far less likely for “imposters,” who know from the start who their friends and enemies are, to impose double roles on themselves. As will be seen in this paper, the act of assuming double roles usually occurs after some important information regarding the enemy identity is revealed to them, allowing them to make some forms of “contracts” with the pre-assigned enemies.

III. VARIATION OF SOCIAL DEDUCTION GAMES AND THE FIRST EXAMPLE

It may perhaps turn out that online social deduction games, with their associated virtual multiverses and maps, can remind us of our own dream worlds. In some cases, actions taken in dream worlds can be intentionally or inadvertently performed in reality because they express certain psychological facts and relationships (Rank, 2012). These expressions vary from game to game. On the one hand, in “Among Us”, verbal discussion is only allowed in the meeting where voting takes place to eliminate suspicious players. On the other hand, in “Goose Goose Duck” and “Deceit 2,” verbal interactions are allowed outside the meeting or voting phase and can be achieved locally or sometimes remotely under some special conditions.

Capability of verbal interactions allow players to describe or receive (sometimes fake) information, thus facilitating their understanding or misunderstanding about the situational reality. Streaming social deduction games attract viewers’ attention because it parallels what they learn from real life regarding how to successfully convey information or deceive people.

First, let us try to capture what MRYEARN was thinking and interacting with other players as a goose in an impressive match from “Goose Goose Duck.”

MRYEARN, given the role of a “Lover Goose,” had two ways of winning the game. On the one hand, to win as a “Goose,” he has to eliminate all “Ducks,” mainly by cooperating with other geese to vote the ducks out. On the other hand, he can also win as a “Lover” by surviving until the end only with his lover. Naturally, it is easier to win as a goose and more challenging to win as a lover because of the limited winning condition of only two remaining survivors in the “Lover” case.

After he found out his lover in the game is NONGPAT, he has not much challenging things to do except perhaps to find out all the “Ducks” and other roles, especially the “Pelican.” Then, he was suddenly swallowed by SOMETIMES, the pelican, only to be escaped later after NONGPAT slew SOMETIMES. This scenario let him know that his lover, NONGPAT, was a duck. So, he knew almost every important role in the game, except one remaining duck.

After the escape, he found himself in a scene where NONGPAT the duck, HEART, the fellow escapist, and VIPERDEMON were present.

In this scene, only VIPERDEMON was a truly innocent goose having no idea which ones were his enemy. HEART was indeed a duck. To prove to NONGPAT that he was a duck and not a “Mimic Goose,” HEART killed VIPERDEMON and revealed himself such that all remaining three players in the scene knew one another’s roles.

Figure 1: Goose Goose Duck Scene After MRYEARN and HEART Escaped From The Pelican's Belly
Source: HEARTROCKER (2024)

MRYEARN was initially astonished with HEART's revelation which left him a sole goose accompanied by two ducks. However, he suddenly detached himself from the assigned role of goose. He announced that from now he would help the ducks win, thus creating an alter ego which cannot be described by any of the game's official roles.

After this scene, MRYEARN strictly played along with his new self-imposed role, brainstorming and cooperating with the two ducks like he was one of them, except that he could not kill.

Figure 2: Goose Goose Duck Scene After HEART Killed VIPERDEMON And Implicitly Revealed His Role
Source: HEARTROCKER (2024)

Figure 3: Goose Goose Duck Cutscene with Ducks' Victory
Source: HEARTROCKER (2024)

The ending cutscene showing HEART and NONGPAT as victorious ducks came after the meeting where MRYEARN cooperated with ducks to eliminate CONNUAY, thus leaving him and DISTROTION as only two remaining (official) geese, satisfying ducks' winning condition.

MRYEARN lost the game as a lover goose, but, according to his self-imposed role, he won.

IV. THE SECOND GOOSE GOOSE DUCK EXAMPLE AND COMPARISON WITH THE FIRST

In specific cases studied in this paper, we need to analyze for the meaning of double roles in order to understand complicated player strategies. This can be achieved by tracing the player motifs in game streaming and comparing the observed formations with one another as well as psychological literature. We should be able to clearly see how these motifs originate from individual concepts in the mind of game streamers who are psychologically disposed to them.

In Thailand's streaming community, there is not much doubt that "HEARTROCKER" (named as "HEART" in the previous game example) gives much streaming inspiration to his successor and audience. He is seen as the classical content creator of many online games, in which his social deduction game streaming is one of the most popular with more than a million YouTube views per video.

Figure 4: Ending Cutscene With Lovers' Victory
Source: HEARTROCKER (2023a)

From observation, none of HEARTROCKER's social deduction game streaming is entirely free of our double roles concept. Another example is taken from the 19th gameplay from the game "Goose Goose Duck," streaming on September 15, 2023, with the video title "Playing Ducks First Time in Many 20th Anniversaries."

The gameplay bears similarity with the previous example. HEART, the lover goose, met CONNUAY, the lover duck from the very start of the game. CONNUAY let HEART know from the start that he is a duck. HEART decided to cooperate with CONNUAY, apparently never considering about winning as just a goose. Note that had HEART betrayed and CONNUAY been voted out, HEART could still have won even when he died. However, HEART decided to join CONNUAY, walking together the entire game as the partner of the crime, witnessing CONNUAY murdering other geese while lying and giving false alibi. At the end of the game, all other players are eliminated such that they win together as lovers.

For the sake of relevance, we will indicate here briefly about the essential correspondencies and parallels, and also some differences, from our two examples discussed so far. Just as in MRYEARN's case in the previous example, this example is also the case in which the lover goose (HEART) bargains with his own soul and form a pact with the villain (Duck).

Although, suddenly after the game ends, the general feeling expressed by other losing players in the two game plays are quite different, the feeling of audience watching the streaming is similar. They particularly enjoy both gameplays more than others in the same game streaming. Some called it "MVP" (Most Valuable Play) in YouTube's comment section. Indeed, even if MRYEARN himself officially lost, he was proud of himself for helping the Ducks win, as he remarked "I did not actually win but I felt I won anyhow."

As for the losing players' reaction, in the first example, they were at first nothing but slightly disappointed, because they did not know how MRYEARN helped the ducks win. However, they became more interested during the discussion thereafter. This contrasted with the second example where the lovers won. They were unanimously amazed since the victory as lovers rarely happened.

V. THE DRAMATIC THIRD EXAMPLE: DECEIT 2

One of the most formal, explicit, and profound treatment of double roles in social deduction games is found in the streaming of a famous social deduction game called “Deceit 2.” The game portrays the effort from the “Innocents,” being chased and persecuted by the “Infected,” to escape the “Ritual.” Within the “Ritual,” time is divided into “Reality” and “In-Between.” In the “Reality” phase, the innocents and the infected look-alike. The innocents may not be aware of the infected’s existence until the in-between phase breaks out. In this state, a nice fellow during the reality phase can transition into “Terror,” a horrific creature that hunts down and execute the innocents, who have to survive this phase until the reality returns. The phases will alternate until all innocents are killed and the infected win, or all infected ones are eliminated in the reality phase and innocents win. Also, if the innocents find the key, they might escape together even when the infected are not yet eliminated.

The development of our example’s story from the start to the catastrophic end of our streaming protagonist HE5 (Nina), who is given the “Guardian” role, are reproduced here in words. Of course, some detail is omitted, as we try to recapitulate briefly.

The unfortunate hero of the story, HE5 (Nina), with his role as a guardian, was determined to make his role beneficial. In the first reality phase, he first met DIP DIP (Alex) and used his role skill to protect him. After that, the two encountered KS139 (Chang) before having a fistfight with one another. Irritated by his two companions, HE5 continued on his own and then noticed ZYLNAZTER (Beck) drinking blood at a blood altar. ZYLNAZTER asked HE5 to stay quiet and tell no one about what he saw. Otherwise, his role as an infected would be revealed.

Figure 5: ZYLNAZTER Drinking Blood From The Blood Altar
Source: HEARTROCKER (2023b)

Both made a bargain. HE5 promised to tell nobody if ZYLNAZTER told another infected one not to hurt him. The contract seemed unavoidable, so ZYLNAZTER agreed. When the first in-between arrived, HE5 was

walking together with ZYLNAZTER, who then transformed himself into a gigantic terror form. ZYLNAZTER attacked other innocents but kept HE5 safe.

With every innocent being safe after the first in-between, the next reality phase came and HE5 was joint by KS139 and 1000PRUENI. The reality ends quickly and the second in-between entered. Being convinced he would be sparred by the infected. HE5 roamed the Ritual carelessly but found himself attacked by a terror. He managed to escape and reprimanded the terror, reminding it about the contract made between him and ZYLNAZTER. While this happened, one innocent was killed somewhere else in the map and the reality returned.

Figure 6: Terror Attacking HE5
Source: HEARTROCKER (2023b)

In this third reality phase, HE5 ran into KS139. Having a gut feeling that KS139 was the terror attacking him, he made an accusation and KS139 easily confessed. Still angry about the previous attack, with ZYLNAZTER present, he told some other innocent that ZYLNAZTER was the infected who broke the contract. Then, the third in-between arrived.

In-between should be the time when the infected chase the innocence. However, when the contract with the evil was made and partly broken, HE5's de facto role now was not really the innocent. He now engaged in a heated discussion with the two infected players regarding the attack in the last phase. ZYLNAZTER acted as if he was very guilty and blamed KS139 for breaking the contract. The broken contract tormented him to the point that he challenged his fellow infected, KS139, to a bare-handed duel. The streaming viewers found themselves in a hilarious scene where two gigantic terrors got into a fistfight while HE5 witnessed. Unfortunately, during the fight, HE5 was caught by accident and ended up dead.

The last reality phase in the game ended in chaos as ZYLNAZTER, filled with grief and guilt at HE5's death, confessed he was the infected. There are fistfights all around. Eventually, ZYLNAZTER and KS139 was voted out. The innocents won.

Figure 7: Two Terrors' Fistfight
Source: HEARTROCKER (2023b)

VI. CONCLUSION

From our three examples, apart from the contracted double roles, which might take various forms as Lover Goose-Duck or Innocent-Infected, all these gameplays exhibit a series of coinciding motifs so noticeable that it seems hardly necessary to call special attention to them once again. If the two parties strictly follow the contract, the gameplays may look funny to the streaming viewers but at least the end can be viewed as smart strategic maneuvers. However, as seen in the last example, possible conflict of interest can lead to a catastrophic drama resulting in the loss of the parties involved. The game situation could look chaotic and confusing. However, viewers like it and find it hilarious, as seen in the video streaming's comment section.

Taking notice of the double roles pattern implemented by different streamers and loved by viewers, some attention should be called to their similar underlying psychological structures. We intend to look at them more closely in detail in future work.

REFERENCES

Eger, M., & Martens, C. (2018). Keeping the story straight: A comparison of commitment strategies for a social deduction game. In J. Rowe & G. Smith (Eds.), *Proceedings of the 14th Conference on Artificial Intelligence and Interactive Digital Entertainment Conference (AIIDE 2018)* (Vol. 14, No. 1, pp. 24-30). PKP Publishing Services Network.

HEARTROCKER. (2023a). *"Goose Goose Duck" game in twenty years*. https://www.youtube.com/watch?v=PbtLhGE9FsY.

HEARTROCKER. (2023b). Gathering of the actors | Live - Deceit 2 - Part 3. https://www.youtube.com/watch?v=z8OIEUEvPgs.

HEARTROCKER. (2024). *Goose Goose Duck 2024 (This Live is all ducks).* https://www.youtube.com/watch?v=8qkCJU0ekMI.

Kopparapu, K., Duéñez-Guzmán, E. A., Matyas, J., Vezhnevets, A. S., Agapiou, J. P., McKee, K. R., Everett, R., Marecki, J., Leibo, J. Z., & Graepel, T. (2022). *Hidden agenda: A social deduction game with diverse learned equilibria*. In *the 35th Conference on Neural Information Proceeding Sydstems (NeuralPS 2021)* (pp. 1-11). Cornell University.

Rank, O. (1989). *Art and artist: Creative urge and personality development*. Norton.

Rank, O. (2012). *The double: A psychoanalytic study*. UNC Press Books.

Wiseman, S., & Lewis, K. (2019). What data do players rely on in social deduction games? In J. Arnedo & L. E. Nacke (Eds.), *the CHI PLAY'19 Extended Abstracts: Extened Abstract of the Annual Symposium on Computer-Human Interaction in Play Companion Extended Abstracts (SIGCHI)* (pp. 781-787). Association for Computing Machinery.

IJIET
INTERNATIONAL JOURNAL
OF INDUSTRIAL EDUCATION AND TECHNOLOGY
ISSN 2673-0448

Book Review

BOOK REVIEW: DESIGNING EFFECTIVE INSTRUCTION (7TH EDITION), 2013 GARY R. MORRISON, STEVEN M. ROSS, HOWARD K. KALMAN, AND JERALD E. KEMP

Reviewer: Thahdarphut Limapornvanitr*
Email: thadharphut.li@kmitl.ac.th*

Received: April 4, 2024
Revised: June 10, 2024
Accepted: July 12, 2024

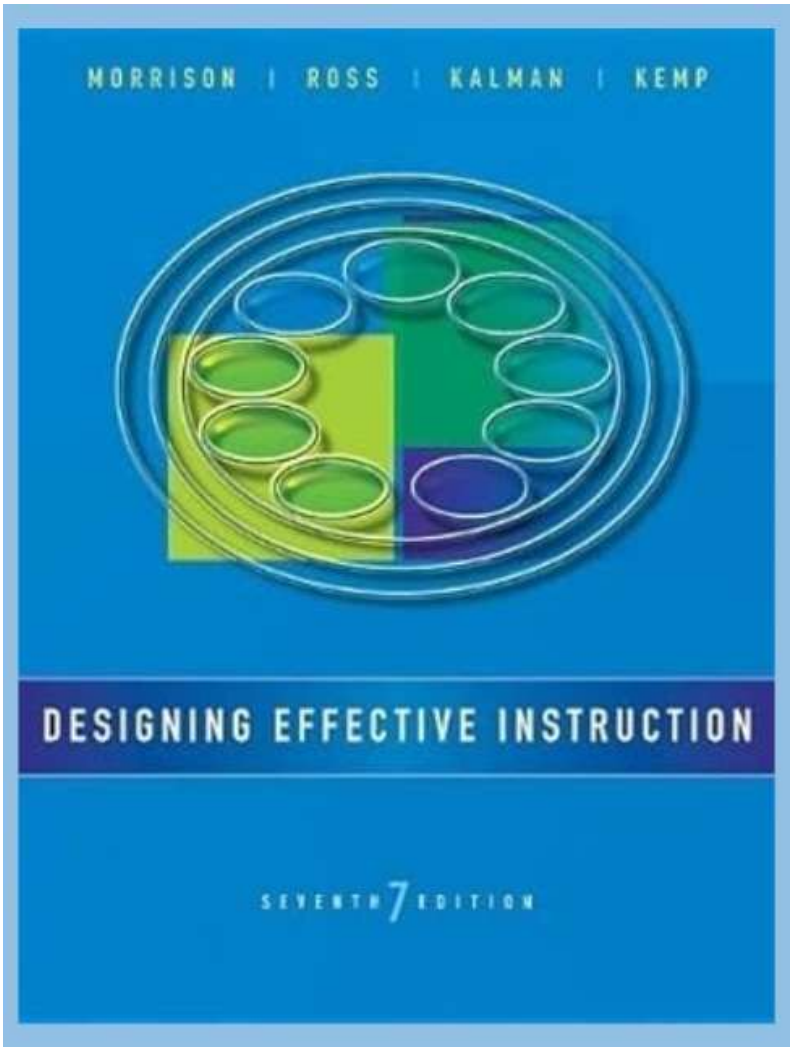

*Corresponding author E-mail: thadharphut.li@kmitl.ac.th
Department of Architecture Education and Design, School of Industrial Education and Technology,
King Mongkut's Institute of Technology Ladkrabang, Bangkok 10520 Thailand

ABSTRACT

Instructional Design (ID) is a systematic approach to creating effective learning systems closely tied to instructional technology. Popular systematic models of Instructional Design include Gagne's nine events of instruction, introduced in 1961, and five tasks from comprehensive learning frameworks. These models combine teaching approaches with learning theories to enhance learner development and achieve desired learning outcomes.

Effective Instructional Design incorporates thematic analysis to address factors contributing to a practical e-learning experience. Well-crafted instructional designs can stimulate learners' cognitive structures, making learning more effective. Both instructors and instructional designers need to understand the demands of the instructional design process. Quality learning experiences result in achievements encompassing knowledge, skills, and attitudes.

Keywords: Systematic instructional design, Instructional design model, Instructional model,

Introduction:

Designing Effective Instruction is based on the work of Jerrold E. Kemp, who started his career as a professor at San Jose State University in California. In 1971, he published his first book, "Instructional Design: A Plan for Unit and Course Development". This book provides essential knowledge about instructional design and outlines the process, emphasizing its purpose and importance in educational contexts. In Figure 1, Kemp's instructional model is flexible and adaptable to various disciplines and learning styles. He stresses that the learning experiences created for students should be challenging, engaging, and rewarding. His model features a nonlinear, circular structure, illustrating that the design process is an ongoing cycle. A well-crafted instructional model based on Kemp's approach must include continuous planning, design, and evaluation to ensure high-quality instruction.

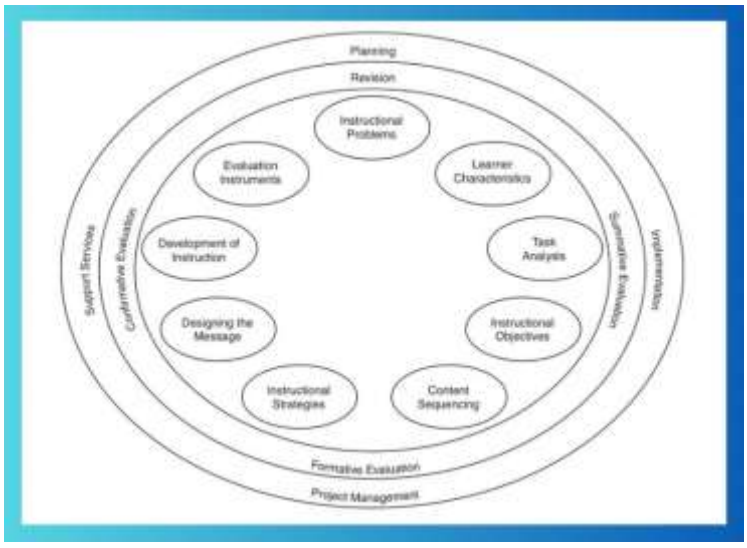

Figure 1: Component of the instructional model plan (Morrison, Ross, Kemp, 1971)

Book Structure:

The field of instructional design began to take shape during World War II. This article discusses the origins and development of instructional design, highlighting shifts in theoretical approaches, particularly those related to behaviorism and cognitive psychology. It focuses on contemporary theories, research, methodological challenges, and potential future directions.

Instructional design involves creating structured learning plans that effectively deliver educational experiences. The primary goal is to develop the skills and knowledge that learners need to acquire. Instructional designers draw on academic theories and models to better understand how people learn and the cognitive processes involved in learning. These instructional models ensure that teaching methods are as effective as possible for imparting knowledge and teaching skills. Instructional design (ID) refers to the systematic and professional planning of education or training. ID is interconnected with instructional technology, instructional science, and educational psychology. The evolution of instructional design has been driven by two key factors: first, the duration of training, which influences how much time learners need to acquire knowledge; and second, the necessity of using efficient instructional methods. These methods can include various media options, such as written instructions, demonstration videos, and hands-on exercises. (Morrison et al., 2013).

Designing Effective Instruction (Morrison, Ross, Howard, and Kemp, 2013) is a comprehensive textbook that presents a flexible framework for instructional design based on the model by Morrison, Ross, and Kemp. This book is intended for instructors, educators, graduate students, and anyone involved in education. It is also valuable for those looking to adopt instructional design models for corporate organizations. The book is divided into three main sections. First, it is organized into fifteen chapters. The initial chapters cover the instructional design process, including an introduction to instructional design, analysis of instructional needs, learner and contextual analysis, task analysis, setting instructional objectives, designing instructional strategies, sequencing content, and developing instructional messages. The tenth chapter specifically addresses the use of technology in instruction.

The second section focuses on evaluation, compiling various types of assessments and illustrating the relationships between them. These chapters emphasize the importance of the validity and reliability of tests and their interrelationship. The third section includes chapter twelve, which outlines the process and criteria for developing evaluation instruments, and chapter thirteen, which demonstrates how to implement these instruments within a learning program. Chapter fourteen explores learning and instructional theory, while chapter fifteen explains how to implement instructional design effectively. Additionally, several instructional models have been developed and integrated into learning processes. The final chapter, Instructional Design Project Management, covers essential aspects of implementing instructional learning models in projects. The appendix contains collections of instructional design model documents and examples of instructional units.

The seventh edition of this book was released in 2013 and consists of 16 chapters. Instructors have the flexibility to adapt the chapter sequence to create a class learning plan that aligns with their teaching approach. The editorial team developed this book based on feedback and ideas from their colleagues. Each chapter begins with an introductory section that provides real-world scenarios related to the chapter's topic. This is followed by relevant content and essential information on the main subject. The section on practicing instructional design shares insights, successes, and perspectives from real-world situations, often introduced through an interactive presentation. The content of each chapter is organized with an introduction and guiding key inquiries that help readers navigate essential issues. All related processes of instructional design

are explained in various ways, with detailed discussions on how these processes have been applied and the elements of the model involved. At the end of each chapter, there are exercises designed to test readers' skills, concluding with professional feedback on instructor decisions and choices.

This book emphasizes the cohesive nature of a learning model that can adapt to basic skills and be applied in various contexts, including multimedia, traditional classrooms, and distance education. It serves as a valuable theoretical resource in the fields of education and educational technology. In today's digital era, educational technology is essential for enhancing learning experiences and preparing students for the future. It utilizes a variety of tools and applications to improve teaching and learning across different academic environments, ranging from traditional classrooms to online learning spaces. During the COVID-19 pandemic, educators adapted by utilizing online tools to effectively facilitate quality distance learning. As a result, technology has become an integral part of classroom instruction, whether in-person or online, across all educational levels. The field of educational technology is rapidly evolving and expanding. Instructional designers leverage educational technology to create curricula that equip organizations with information, skills, or practices. Instructional design is a systematic process that connects teaching strategies with technology, making it easier to implement technology that simplifies complex concepts.

Reflection:

This method of instructional design customizes learning approaches by integrating technology into online courses. By taking into account learning goals and student needs, a well-designed classroom can promote interactive learning environments that strengthen connections among learners, instructors, and the content, thereby enhancing effective learning. Utilizing instructional design models can greatly improve the overall learning experience. These models help bridge the gap between content and learning outcomes, establish appropriate objectives, and create interventions that enable participants to achieve their learning goals.

An engaging textbook helps users understand instructional models by connecting concepts to relatable, everyday examples and using language that is easy for everyone to understand. To enhance comprehension, clear diagrams paired with straightforward explanations significantly boost the instructor's engagement from the start. Sharing expert insights alongside real-world experiences in instructional design links theory to practical application. This book is consistently updated in each edition, ensuring it remains a valuable and current resource. The structured presentation of supportive information enhances confidence and clarity for beginners in instructional design. Instructors gain a comprehensive understanding of the instructional design processes, allowing them to effectively organize their instructional model framework. Effective instructional models lead to greater learning outcomes and can inspire practitioners to innovate their instructional design approaches. The implementation of these models can be beneficial in both academic education and training programs.

Conclusion:

Designing Effective Instruction (7th Edition), published in 2013, encompasses various settings, including technology, to enhance instructional design and foster student learning. The book emphasizes the unity of the instructional design model, providing a solid foundation of knowledge while improving essential skills. All chapters have been updated to reflect recent trends and research. This practical resource offers impactful and adaptable frameworks that connect to various academic fields and industries.

REFERENCES

Morrison, G. R., Ross, S. M., Kalman, H. K., & Kemp, J. E. (2013). *Designing effective instruction* (7th ed.). John Wiley & Sons.

IJIET
INTERNATIONAL JOURNAL
OF INDUSTRIAL EDUCATION AND TECHNOLOGY
ISSN 2673-0448

Research Articles

STUDY UNIQUENESS OF MARIGOLD FLOWERS TO DESIGN WOMEN'S BAGS ACCORDING TO THE CONCEPT OF CREATIVE ECONOMY

Somchai Seviset*, Supinyo Wongphame, and Mallika Yimcharoen
E-mail: somchai.se@kmitl.ac.th*, wongphame@yahoo.com, 64030152@ kmitl.ac.th

Received: 15 March 2024
Revised: 24 May 2024
Accepted: 31 July 2024

ABSTRACT

This research aims 1) to study the characteristics and shapes of calendula used for the design of bags for women, 2) to design women's bag products based on marigold patterns, and 3) to evaluate the satisfaction of consumers with the product. Research methods to design bags from marigold patterns with a population group of women in Lat Krabang District, the population statistics, obtained from the house registration office level in Lat Krabang District, Bangkok, for the year 2023, were 16,123. The sample group comprises women from Lat Krabang District. Bangkok (Population Statistics from House Registration, Registration Office Level, Area, Lat Krabang District, Bangkok, 2023) with confidence of 95 percent by randomly sampling 35 people. The researcher studied the observed variables and measured the 5-level Likert rating scale for 10 questions, assessing the quality of the research instrument by considering the accuracy of the questionnaire in relation to the question and the objective. The research revealed that the level ($\overline{X}$ =4.76; SD= 0.40) had the highest level of satisfaction, ranking from first to third in terms of product satisfaction. The second place is that the product has strength and durability at the level ($\overline{X}$ = 4.91; SD = 0.28), and the third place is that the product has bright colors that match the characteristics of the marigolds at the level ($\overline{X}$ = 4.71; SD = 0.45).

Keywords: Marigold patterns, Calendula, Women's Bags, Creative Economy

*Corresponding author E-mail: Somchai.se@kmitl.ac.th
Department of Architectural Education and Design, School of Industrial Education and Technology
King Mongkut's Institute of Technology Ladkrabang, Bangkok 10520 Thailand

I. INTRODUCTION

In today's rapidly evolving global and fiercely competitive economy, companies need to innovate continuously. Innovation is now recognised as one of the most successful strategies for profitable growth, capturing market share, and even the means of surviving (Hamel, 1998, pp.7-14). Product innovation is a key factor of enterprise innovation, and creative design is the core of product innovation.

How do designers conduct a creative design? What factors affect creative design? How could designer's creativity be enhanced? Many researchers all over the world have done a great deal of work from different perspectives of knowledge (Benami & Jin, 2002, pp. 251-263; Hori, 1997, pp. 29-35; Kitamura et al., 2004, pp. 115–127; Richards & Simoff, 2001, pp. 121–136; Watson & Perera, 1997, pp. 59–87), psychology (Hsiao & Chou, 2004, pp. 421–443; Thompson & Lordan, 1999, pp. 17–31) and theory of inventive problem solving. However, those methods still have such-and-such limitations for carrying out creative design practically. Moreover, tradi-tional design methods mainly focus on products or technical systems themselves and seldom recognise and plan the design process from the viewpoint of creative cognition approach.

The purpose of this research was to study the shape characteristics of marigolds used for the design of women's bags to design women's bags from marigold patterns and to evaluate the satisfaction of consumers with women's bags from marigold patterns. For use in the design of product patterns on bags, consumer data is studied, including: 1. Study information about the characteristics of marigolds. 2. Study the behavior of buying bags. 3. Learn about the bag. 4. Learn about the bag's material. 5. Study the design principles, and 6. Study related research.

Moreover, by 2025 in the market of bags, backpacks, bags and luggage in the downstream market, the demand for women and men is almost the same. While in high-end markets with higher purchasing power, female consumers are prominent, and the trend of market development should be eco-friendly style is becoming more and more popular. The research for this product design stems from the issue that no marigold patterns have been created before, despite the marigold flower's significant role in Thai culture and its status as the royal flower of His Majesty the King. Because the marigolds are bright yellow to match "Monday," which is the day of His birth, it is like His beautiful life.

These problems have had a negative impact on the population in Thailand lacks detailed knowledge about marigolds, and if these issues are not addressed, it will negatively impact consumers. The population in Thailand will still know the importance of marigolds.

In summary, if this research is successfully conducted, it will benefit consumers by enhancing their satisfaction with usability and aesthetics. Marigold bags and the social benefits of creating new patterns have inspired people in society and the economy to create new women's bags. Therefore, the researcher and product creator have conducted systematic research to find an industrial product model that is suitable and in line with consumers' needs and the context of the problem.

II. CONCEPTUAL FRAMEWORK

2.1 The researcher uses a conceptual framework in design with the principles of product design (Saribut, 2007, pp. 18-19). There are 12 points, and the researcher has applied only 4 points in this research: (1) aesthetics; (2) material; (3) durability; and (4) usability by applying the principles of design elements to the product design process.
Marigold Pattern Bag

2.2 The researcher used a conceptual framework to assess consumer satisfaction with the newly designed product. The buyer decision-making process (Kotler and Armstrong, 2011, pp. 79-82) includes (1) problem/need recognition, (2) information search, (3) evaluation of alternatives, (4) purchase decision, and (5) post-purchase behavior.

III. RESEARCH METHODOLOGY

3.1 The research method for objective 1 involves examining the characteristics. The researchers studied the botanical characteristics of marigolds and designed bags from marigold patterns according to the details of the research process. as follows.

a) The variable studied was the level of satisfaction of women in Lat Krabang District, Bangkok

b) The population group is a group of women in Lat Krabang District, Bangkok (Population Statistics from House Registration, Registration Office Level, Area, Lat Krabang District, Bangkok, 2023) 16,123

c) The sample group is a group of women in Lat Krabang District, Lat Krabang District. We used Robert V. Krejcie and Earyle W. Morgan's (1970) formula for figuring out the number of samples (Krejcie & Morgan, 1970, pp. 607–610) to find the confidence level at 95% by picking 35 people at random (accidental sampling).

d) Research tools, such as questionnaires, are utilized to study the content. The Ranting Scale is a tool used by researchers to collect data from samples of people.

e) Data analysis is the analysis of documents by systematic review (SR) and descriptive statistics by determining frequency, percentage, mean, and standard deviation (SD), etc.

3.2 Method of conducting research objective 2 To design bags for women from marigold patterns, the researcher evaluated consumer satisfaction with the design of bags from marigold patterns according to the details of the research process. as follows.

a) The primary variable is a bag product made from a newly designed prototype marigold pattern.

b) The population group is a group of women in Lat Krabang District, Lat Krabang District. Bangkok Province: 16,123 people

c) The sample group is a group of women in Lat Krabang District, Lat Krabang District. We used Robert V. Krejcie and Earyle W. Morgan's (1970) formula for figuring out the number of samples to find the confidence level at 95% by picking 35 people at random (accidental sampling).

d) Research Tool: A questionnaire with a satisfaction assessment consisting of 10 assessments in the study of marigold identity for bag design is a 5-level evaluation (rating scale) tool used by the researcher to collect data from a sample.

e) Data analysis involves the determination of percentages, means, and standard deviations (SD), among other descriptive statistics.

IV. RESULTS

4.1 Objective Result 1: By conducting a preliminary data study, preliminary data collection is shown. as follows.

The process involves studying basic information on consumer needs. It was found that consumers have a demand for bag products with patterns that respond beautifully to women's needs. Before designing the product, it should take into account 1) taste, 2) price, and 3) materials used in production, and then use the basic information obtained to analyze it with techniques. Here is a detailed SWOT analysis of three case studies:

a) The first comparative product case study has the following features: 1) The brand is famous. 2) It has a large customer base. 3) It is the only bag with brand print in the world. 4) The bag boasts high-quality materials. The disadvantages are 1) it is expensive, 2) the bag has a strong smell, and 3) the design is quite old. This has led to an increase in options in the market. There are more choices for consumers.

b) The second comparative product case study has the following advantages: 1) Beautiful bag design 2) Meticulous design of patterns and production 3) Affordable and affordable 4) Fine tailoring and beauty The drawbacks include 1) reduced use of color, 2) a smaller customer base, and 3) a lack of brand awareness among customers. 4) The design is quite old. 5) The design emphasizes one that responds to consumers who are quite old. The opportunities include being 1) affordable, 2) catering to a higher consumer income rate, 3) offering multi-channel ordering, 4) offering cheap bags, and 5) offering more than one bag.
2) Consumers prefer to buy branded products from abroad rather than in their own country. 3) Younger consumers (teenagers) are less likely to use this type of bag.

c) The third comparative product case study has the following features: 1) The bags are beautiful; 2) the colors are bright; 3) the color patterns are diverse and novel; and 4) the design is suitable for the style of dress and age range. The opportunities are: 1) There is a variety of bag shapes, 2) it is cheaper than the income level of consumers, and 3) there is a collection. 4) You can order through multiple channels. 5) The bag is cheap; you can buy more than 1 bag. 2) Consumers prefer to buy branded products from abroad rather than in their own country.

Figure 1: Case study with neighboring products compared with SWOT analysis technique.
Source: (Seviset et al., 2023)

2) The process of analyzing and finding solutions to consumer needs with the Quality Function Deployment (OFD) technique reveals 24 problems that need to be solved, and the product researcher has proposed 24 solutions to solve the problems that appear.

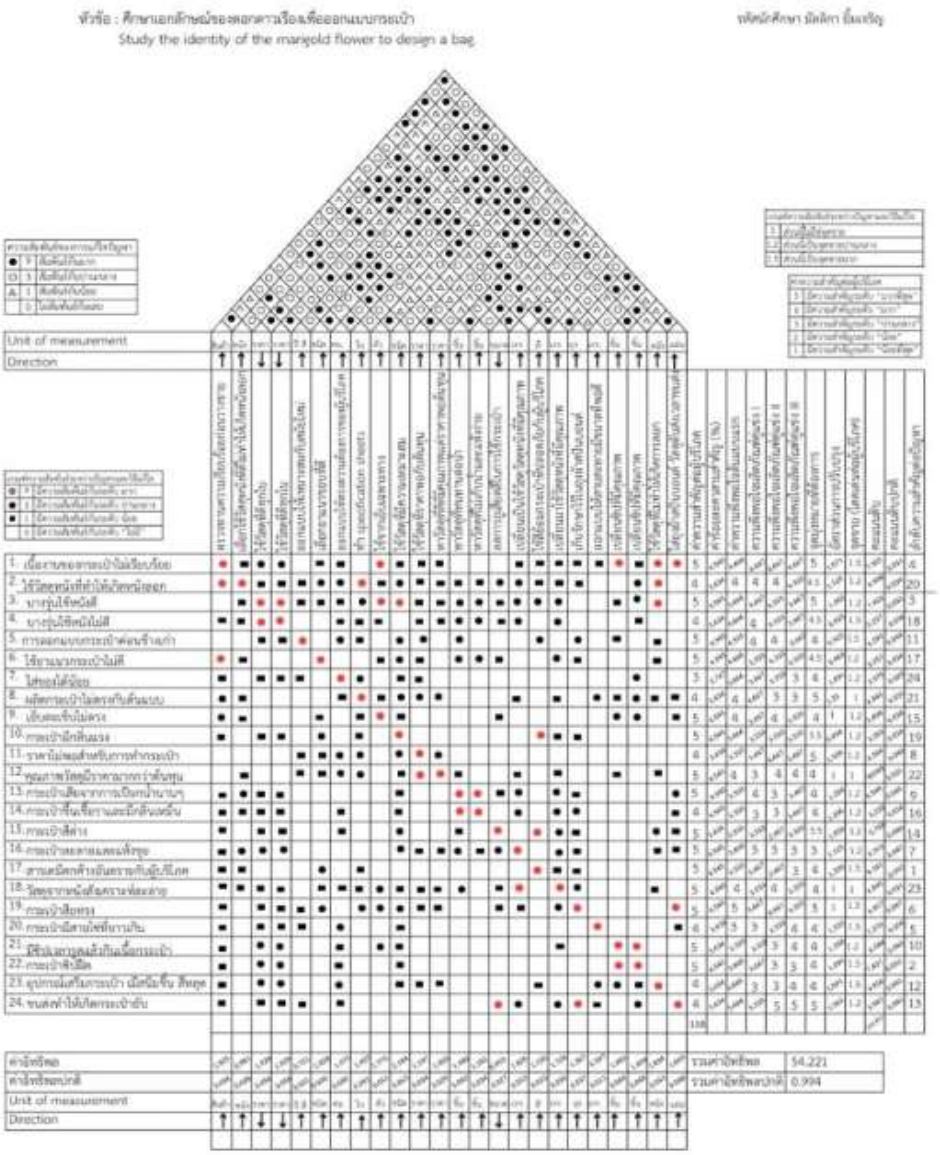

Figure 2: Quality Function Deployment (QFD) Analysis Process
Source: (Seviset et al., 2023)

Using the QFD technique, we identified the first five solutions in descending order.

1) The first major solution is that the bag has a strong smell. Normal Influence Score (0.062).
2) The second major solution is that the bag work is not neat, and the influence score is normal (0.056).
3) The third major solution is that the bag is melted and dried, flaky, and the influence score is Normal (0.034).

4) The fourth major solution is that the bag design is quite old. Normal influence score (0.021).
5) The fifth major solution is that the bag has an excessively long chain and has a normal influence score (0.011).

Then, the researcher created a bag product from a marigold pattern and brought the solution to the problem that consumers want into the creative stage from "abstract problem-solving features" to "concrete problem-solving features" design. To present new product design guidelines with the sample technique,

3) New product creation process with SCAMPER: The researcher presented the results of the analysis and created a new product through fusion. "Problem Solving Guidelines on New Products" enters the product design stage by applying the conclusions of the 24 qualitative function distribution techniques to be refined and applied together before the product design stage. SCAMPER is creating creative ideas classified into 7 creative items.

Figure 3: Creativity based on the SCAMPER concept design concept.Source:
Source: (Seviset et al., 2023)

4) The process of summarizing design results that apply the SCAMPER technique: By integrating the seven principles together, it can show the results of creating or designing a new product. as in the picture of the new design that is integrated in bringing all 7 parts together into a new product model and a new product development image (design development).

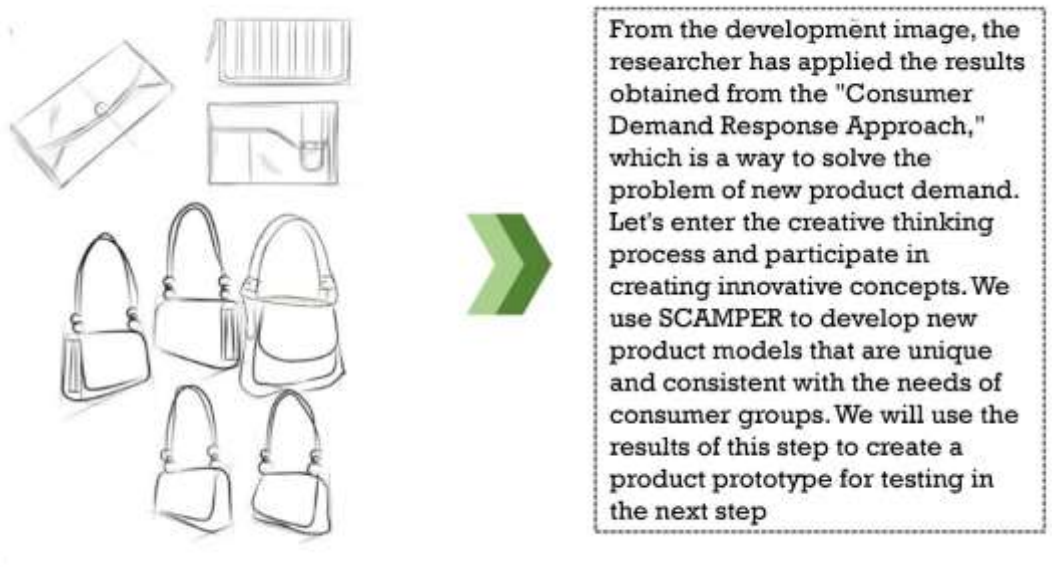

Figure 4: Integrating the 7 parts together into a "new product model" and design development.
Source: (Seviset et al., 2023)

5) The design process of the handbag product features marigold patterns with golden-yellow flowers, whose petals are arranged in a very beautiful and orderly manner (Kasemsap, 2015, pp. 393-394). The researcher presented three sketch design concepts to showcase ideas that integrate problem-solving approaches derived from the application of QFD and SCAMPLE analysis techniques. This development of a stematic creative thinking approach involved organizing the design thought process as follows:

Figure 5: Sketch the design of three styles of bag products from Marigold patterns.
Source: (Seviset et al., 2023)

6) The process of producing a prototype of a bag product from a marigold pattern by the researcher and creator has carried out the prototype production with the following steps: 1) Step 1: Product sketch step, 2) Product material search stage, 3) Pattern screen stage. 4) The production process of bags, etc., by which the researcher can present a prototype image of the finished product. as follows.

Figure 6: A prototype of a bag product made of a marigold flower pattern.
Source: (Seviset et al., 2023)

7) The trial process was conducted by a consumer group, specifically the women's group in Lat Krabang District. Bangkok Province When consumers use it, it appears that the product is suitable and in line with their needs. The appropriate application process expresses this. It can show how consumers use the prototype product. as follows.

Figure 7: Shows the application of a consumer product prototype using sesame in real-world settings.
Source: (Seviset et al., 2023)

Summary of the results of the study on the design and creation of bag products from marigold patterns. The design study revealed facts derived from testing a new prototype product using the SWOT analysis technique. Newly developed prototype products include:

a) The highlights of the new product include: 1) product aesthetics and style bag 2) Unique pattern 3) Easy to care for and durable.

b) Disadvantages of new products include: 1) Less storage compartment

c) Opportunities for new products include: 1) Patterns, 2) Fashion trends, 3) Novelty.

d) Risks of new products include 1) taste and 2) competitors.

4.2 Objective Result 2: The prototype product is used to evaluate the level of consumer satisfaction, including: 1. The product has bright colors in line with the characteristics of marigolds. 2. The product has beautiful patterns. It shows the uniqueness of marigolds appropriately. 3. The product's shape makes it suitable for both holding and crossbody use. 4. The product's material is easy to clean. 5. The product's material is safe for consumers. 6. The material of the product can prevent wetting. 7. The product is strong and durable. 8. The product has a strong bag structure and does not deform the bag. 9. The number of compartments in the bag is appropriate. 10. Personality enhancement comes from evaluating the level of consumer satisfaction after using a new product. Data is collected from a quality-structured questionnaire, adhering to the specified benchmarks. The results of the satisfaction level are shown in Table 1.

Table 1: Results of Satisfaction Evaluation of New Prototype Product Bags from Marigold Pattern.

Number	Satisfaction Assessment List	$\overline{X}$	SD	Rank
1.	The product has a bright color, in harmony with the appearance of marigolds.	4.71	0.45	6
2.	The product has a beautiful pattern. It shows the uniqueness of marigolds appropriately.	4.94	0.23	1
3.	The product has a shape that is suitable for holding and cross bodying.	4.74	0.44	5
4.	The product's material is easy to clean.	4.66	0.47	8
5.	The product's material is safe for consumers.	4.86	0.35	3
6.	The product's material is resistant to wetting.	4.63	0.48	9
7.	The product is strong and durable.	4.77	0.42	4
8.	The product has a strong bag structure and does not deform it.	4.91	0.28	2
9.	Inside the bag, there are appropriate compartments.	4.71	0.45	6
10.	Personality enhancement	4.69	0.46	7
	Results of the satisfaction level of the New Products in overall	4.76	0.40	Most satisfied

The order of the evaluation items that received the highest satisfaction was determined based on the results of the evaluation of the level of consumer satisfaction.

The product ranks are:

No. 1 place in terms of products with beautiful patterns. ($\overline{X}$ = 4.94; SD = 0.23).

No. 2 in terms of durability ($\overline{X}$ = 4.91; SD = 0.28).

No. 3 in terms of product materials it is safe for consumers. ($\overline{X}$ = 4.86; SD = 0.35).

No. 4 has a robust bag structure that prevents the bag from deforming ($\overline{X}$ = 4.77; SD = 0.42).

No. 5 in terms of product shape suitable for holding and cross-body ($\overline{X}$ = 4.74; SD. = 0.44).

No. 6 place in terms of bright colors, in line with the characteristics of marigolds ($\overline{X}$ = 4.71; SD= 0.45) and the inside of the bag has a reasonable number of compartments ($\overline{X}$ = 4.71; SD = 0.45).

No. 7 place in personality enhancement ($\overline{X}$ = 4.69; SD = 0.46).

No. 8 in terms of materials that are easy to clean ($\overline{X}$ = 4.66; SD = 0.47).

No. 9 in terms of wet-resistant materials ($\overline{X}$ = 4.63; SD = 0.48).

Therefore, from the research process in the design of bag products from marigold patterns, it can be concluded that "the newly designed product is suitable and in line with the needs of the consumer group. This design meets the needs of the consumer group in terms of 1) taste, 2) price, and 3) materials used in production, all in a manner that aligns with the research goals.

V. CONCLUSION AND DISCUSSION

The results of the study in Objective 1 to study the characteristics of the shape of the calendula is used for the design of the bag for The results can be concluded that when developing product models with QFD techniques, solutions are found in descending order of the first 3 priorities: 1) The first major solution is to use all good leather models to match the price without causing comparisons. Influence Points (1.929) Normal Influence Score (0.056) 2) The second most important solution is to choose a good edge grout, and if the leather bag is torn, it needs to be replaced; the edges must be painted close to the old color. Influence Points (1.028). The third important solution is to study various plots and apply them in design to suit modern times,

with an influence score value of (0.721) and a normal influence score (0.021, etc.). The researcher then presented 3 sketch design images to present the concept that integrates the solution to the problem obtained from the application of both analysis techniques. In conclusion, a) the highlight of the new product is the pattern, b) the disadvantage of the new product is that it is not suitable for strong sun conditions, which will make the bag color pale easily. c) The opportunity of a new product is a fashion trend, d) the risk of a new product is a taste, etc. The results can be discussed that the results carried out by the researcher in the design stage are consistent with the concept of Saribut (2007, pp. 18-19). The results of the study in Objective 2 to design women's bag products from marigold patterns showed that the most satisfied consumers rated the highest to lowest satisfaction levels in 5 orders: 1st place in terms of products with beautiful patterns; it shows the uniqueness of marigolds appropriately. The most satisfied level is 2nd place in terms of product strength and durability, the most satisfied level is 3rd place in the product with bright colors, in line with the appearance of calendula, the most satisfied level. 4th place in the material of the product is easy to clean. The highest level of satisfaction. The 5th place in the material of the product can prevent water wetting, the most satisfactory level of satisfaction, etc. The results of the satisfaction level are in line with the concept of Saribut (2007, pp. 18-19). (1) aesthetics; (2) material; (3) durability; and (4) usability. The results of the study in Objective 3 The research revealed that the level ($\overline{X}$ =4.76; SD= 0.40) had the highest level of satisfaction, ranking from first to third in terms of product satisfaction. The second place is that the product has strength and durability at the level ($\overline{X}$ = 4.91; SD = 0.28), and the third place is that the product has bright colors that match the characteristics of the marigolds at the level ($\overline{X}$ = 4.71; SD = 0.45).

This study provides a solid theoretical foundation and a well-structured product design process. The results indicate that a marigold-patterned bag has strong consumers appeal, particularly in aesthetics and durability. However, to successfully launch this product commercially, it should improve material durability to prevent fading, enhance functionality by adding storage space, analyze fashion trends to ensure market relevance, and evaluate production costs for a realistic pricing strategy.

SUGGESTION

The design and creation of bags with marigold patterns have revealed that the newly developed products have weaknesses identified through SWOT analysis, which are 1) the bag colour fades easily and 2) there is limited storage space. If other product designers wish to create new designs, they should consider the aesthetics of the bags and their pricing. It should consider the approach of making the size more universal and increasing storage space and risk. From the SWOT analysis, these are 1) taste and 2) competitors. If other product designers have the desire to redesign, they should consider the approach of studying fashion trends each year and consumer demands each year. The researchers and creators of the marigold-patterned bag hope to benefit consumers in the future.

REFERENCES

Benami, O., & Jin, Y. (2002). Creative stimulation in conceptual design. In *International Design Engineering Technical Conferences and Computers and Information in Engineering Conference* (Vol. 3624, pp. 251-263). ASME.

Hamel, G. (1998). Opinion: Strategy innovation and the quest for value. *Sloan Management Review, 39*(2), 7-14.

Hori, K. (1997). Concept space connected to knowledge processing for supporting creative design. *Knowledge-Based Systems, 10*(1), 29-35.

Hsiao, S. W., & Chou, J. R. (2004). A creativity-based design process for innovative product design. *International Journal of Industrial Ergonomics, 34*(5), 421-443.

Kasemsap, S. (2015). *Agricultural marigolds: Innovative agriculture collection of research innovations on the 72nd Anniversary of Kasetsart University* (pp. 393-394). Kasetsart University. (in Thai)

Kitamura, Y., Kashiwase, M., Fuse, M., & Mizoguchi, R. (2004). Deployment of an ontological framework of functional design knowledge. *Advanced Engineering Informatics, 18*(2), 115-127.

Krejcie, R. V., & Morgan, D. W. (1970). Determining sample size for research activities. *Educational and Psychological Measurement, 30*(3), 607-610.

Richards, D., & Simoff, S. J. (2001). Design ontology in context-A situated cognition approach to conceptual modelling. *Artificial Intelligence in Engineering, 15(*2), 121-136.

Saribut, U. (2540). *Textbook project, Faculty of Education Inudstry.* King Mongkut's Institute of Technology. (in Thai)

Thompson, G., & Lordan, M. (1999). A review of creativity principles applied to engineering design. *Proceedings of the Institution of Mechanical Engineers, Part E: Journal of Process Mechanical Engineering, 213*(1), 17-31.

Watson, I., & Perera, S. (1997). Case-based design: A review and analysis of building design applications. *AI EDAM, 11*(1), 59-87.

Kotler, P., & Armstrong, G. (2011). Principles of Marketing (14th ed.). Prentice Hall.

GPS DELAY TIME AT LOW LATITUDE DURING SEVERE GEOMAGNETIC STORM

Thanapon Keokhumcheng[1], Nitipat Buakao[1], and Chollada Pansong[2*]
E-mail: kthanaponok@gmail.com[1], 66036079@kmitl.ac.th[1], and collada_p@rmutt.ac.th[2*]

Received: September 20, 2024
Revised: October 25, 2024
Accepted: November 22, 2024

ABSTRACT

This study examines the impact of geomagnetic storms on Total Electron Content (TEC) variations and GPS signal delays in low-latitude regions, focusing on the March 24, 2023 (Dst = -163 nT, Kp = 8), and April 24, 2023 (Dst = -213 nT, Kp = 8) geomagnetic storms. Both events, classified as strong geomagnetic storms, significantly affected ionospheric conditions and GNSS signal propagation, particularly in Thailand. The analysis utilized TEC data from three GNSS stations (THCP in Chumphon, THBK in Bangkok, and THCM in Chiang Mai) and revealed substantial fluctuations in TEC and GPS signal delays during the storms. The results indicate that GPS signal delay times increased significantly on the storm days, peaking on March 24 and April 24, before gradually decreasing during the recovery phase. On March 24, 2023, the highest time delay was observed at THBK (10.70 ns), followed by THCP (10.43 ns) and THCM (9.27 ns), whereas on April 24, 2023, the maximum time delay occurred at THCP (9.59 ns), followed by THBK (9.56 ns) and THCM (9.85 ns) respectively.

Keywords: TEC, Delay time, Geomagnetic storm

*Corresponding author E-mail: kthanaponok@gmail.com
[1]Department of Engineering Education, School of Industrial Education and Technology,
King Mongkut's Institute of Technology Ladkrabang, Bangkok 10520 Thailand
[2*]Department of Technical Education, Faculty of Technical Education, Rajamangala University of Technology Thanyaburi,
Pathum Thani, 12110 Thailand

I. INTRODUCTION

The ionosphere is the uppermost layer of Earth's atmosphere, beginning at approximately 60 km in altitude, where solar extreme ultraviolet (EUV) radiation induces partial ionization (Verkhoglyadova et al., 2021, pp. 1-12). This atmospheric layer responds dynamically to solar and terrestrial disturbances, including space weather events. As a crucial transmission medium, the ionosphere significantly affects Global Navigation Satellite System (GNSS) signals, primarily by introducing delays due to variations in plasma characteristics. These disturbances negatively impact GNSS accuracy and reliability in positioning. Free electrons within the ionosphere play a key role in modifying signal properties. Variationsis phase and amplitude are influenced by the Total Electron Content (TEC), which contributes to both signal delays and phase shifts in GNSS transmissions. When plasma is embedded with a magnetic field, it transfers energy into Earth's atmospheric system, leading to noticeable fluctuations in ionospheric parameters such as TEC and the critical frequency of the F2 layer (foF2). These fluctuations manifest as either positive or negative ionospheric storms, depending on whether electron density increases or decreases over a specific period (Zhang et al., 2020, pp. 86-94). During geomagnetic storms, enhanced currents and the influx of high-energy particles generate significant thermal energy within the ionosphere. This heating effect alters atmospheric density, redistributes particles, and increases drag on satellites in low-Earth orbit. The lower-latitude ionosphere exhibits unique variations, including equatorial ionization anomalies and the formation of equatorial plasma bubbles, which pose challenges for ground-based space systems, particularly GNSS and communication technologies (Marini-Pereira et al., 2020, pp. 1-16). The intensification of ionospheric disturbances is driven by factors such as changes in thermospheric wind patterns, ionospheric motion dynamics, and electric fields, all of which contribute to increased electron density. Conversely, adverse storm effects primarily result from alterations in ionospheric composition (Serafimov et al., 1982, pp. 397-399; Chinmaya et al., 2016, pp. 7941-7960; Reddybattula et al., 2019, pp. 283-292). These geomagnetic disturbances lead to fluctuations in TEC, disrupting satellite signal reception and causing delays in signal transmission. Reddy (1986, pp. 247-263), Kumar et al. (2016, pp. 1755-1762), and Jenan et al. (2021, pp. 575-587) found that ionospheric irregularities occur during geomagnetic storms across various latitudes, particularly near the equator and lower latitudes. In these regions, the TEC within approximately ±20 degrees of the geomagnetic equator is higher, leading to greater disruptions in GNSS signal reception compared to other areas. Ionospheric behavior, classified into high, mid, and low latitudes as well as the equatorial region, is influenced by both solar and geophysical factors, resulting in TEC variations during geomagnetic storms (Hofmann-Wellenhof et al., 1992, pp. 1-134; Pi et al., 1997, pp. 2283-2286; Skone and de Jong., 2000, pp. 1067-1071; Chernyshov et al., 2020, pp. 1-13). These TEC anomalies contribute to signal delays, causing positional errors that range from a few meters to nearly 95-105 meters. Plasma density irregularities in the ionosphere distort electromagnetic wave propagation, leading to GNSS signal delays and disruptions in signal paths. The ionospheric layer is vast and exhibits variations in refractive index depending on the signal's operating frequency. To evaluate ionospheric delay, GPS L1 and L2 frequency signals are typically analyzed using frequency combinations and single-frequency ionospheric delay models. Several models have been proposed over the years to predict ionospheric delays, including those by Klobuchar (1986, pp. 280-286), Walker (1989, pp. 68-80), and Coster et al. (1992, pp. 191-204). However, despite advancements in modeling techniques, forecasting ionospheric conditions remains challenging due to the combined influence of terrestrial factors and space-based disturbances.

Several studies have investigated the impact of geomagnetic storms on GNSS performance. For example, Liu et al. (2010, pp. 795-805) analyzed TEC delays and their duration in response to geomagnetic disturbances. Kenpankho et al. (2011, pp. 365-370) compared TEC measurements with IRI models at equatorial latitudes, while Ratnam et al. (2011, pp. 1-6) examined ionospheric delay characteristics at low latitudes during geomagnetic storms. Kenpankho et al. (2013, pp. 1820-1826) further extended their research by comparing TEC measurements with IRI-2007 TEC in low-latitude and equatorial regions. Helmboldt et al. (2015, pp. 387-402) explored the effects of solar flares on the ionosphere at both local and hemispheric levels. Maggiolo et al. (2017, pp. 11,109-11,127) investigated the relationship between geomagnetic activity and delay time occurrences, particularly in connection with solar wind influences. Saito et al. (2017, pp. 1937-1947) analyzed ionospheric delays within Ground-Based Augmentation Systems (GBAS), while Zhang et al. (2018, pp. 1-15) focused on the impact of the ionosphere on GPS delay time. Pan and Guo (2018, pp. 1-17) expanded this research to include real-time delay issues across multiple GNSS systems, including GPS, GLONASS, Galileo, and BeiDou. Ansaria et al. (2019, pp. 248-258) examined TEC fluctuations and compared them with Auto-Regressive Moving Average (ARMA) models and Global Ionospheric Maps (GIM) over Japan. Zhang et al. (2020, pp. 1-16) studied the effects of geomagnetic storms on GPS signal loss in Taiwan. Marini-Pereira et al. (2020, pp. 1-16) mapped ionospheric delays in specific low-latitude regions, while Zhu et al. (2020, pp. 1-14) calibrated GNSS receiver delays using clock-steering characteristics. Sedeek (2020, pp. 1-15) investigated GPS TEC delays during geomagnetic storms over Egypt, and Zhang et al. (2021, pp. 1535-1545) reported TEC time delays during pre-storm and storm conditions in East Asia. Kenpankho et al. (2021, pp. 2152-2159) proposed real-time bias estimation methods for GPS receivers at low latitudes. Lastly, Zhbankov et al. (2022, pp. 194-201) examined the accuracy of satellite positioning systems affected by ionospheric conditions.

Based on data collection and a review of related research, Marini-Pereira et al. (2020, pp. 1-16) analyzed TEC delay maps in low-latitude regions. Their findings revealed that during periods of significant ionospheric activity, errors were typically below four meters in 99.99-100% of cases. On days with minimal ionization, the errors were generally less than one meter. Zhbankov et al. (2022, pp. 194-201) focused on the impact of ionospheric disturbances on GPS accuracy. Instead of relying on traditional techniques such as the Klobuchar model or TEC dependency values to correct ionospheric delays, they proposed a ray-tracing approach within a model designed to more accurately simulate real conditions. This method accounted for various types of Traveling Ionospheric Disturbances (TIDs). Their results demonstrated that large-scale TIDs could introduce errors ranging from 5 to 35 meters, whereas smaller-scale TIDs produced errors of less than two meters. Zhang et al. (2020, pp. 1-16) investigated GPS signal degradation during geomagnetic storms and identified a direct correlation between the maximum GPS signal loss at the receiver and the global average GPS signal's standard deviation. They employed the magnetic geography index to evaluate the severity of GNSS performance disruptions caused by geomagnetic storms. Kenpankho et al. (2021, pp. 2152-2159) examined bias in GPS TEC time delays by analyzing data from a GPS receiver located in a low-latitude region between 2004 and 2019. Their findings indicated that delay times at the receiver were significantly higher on disturbed days compared to calm days. For instance, the highest delay recorded on calm days was 5.8 ns, whereas on disturbed days, it reached up to 6.85 ns, with a minimum delay of 5.3 ns. Additionally, Keokhumcheng and Kenpankho (2025, pp. 4245-4259) compared TEC results obtained from single-frequency GPS with those from dual-frequency GPS, IGS TEC, and IRI TEC in 2023. Their results confirmed that TEC derived from a single-frequency GPS receiver is consistent and reliable for studying TEC delays in the ionosphere over the low-latitude region of Thailand.

After reviewing previous studies on the influence of ionospheric conditions on GPS signal delay, we conducted an investigation into GPS time delays at low latitudes, focusing on the intense geomagnetic storm that occurred on March 24, 2023, and April 24, 2023, over Chumphon, Bangkok and Chiang Mai, Thailand. During this event, significant ionospheric disturbances were observed, impacting satellite communications and GPS signal integrity. Our analysis involved identifying the highest and lowest GPS delay values recorded on the storm day. Additionally, we examined GPS delay times before and after the geomagnetic storm to assess its impact on signal delays, highlighting any significant variations.

II. METHODOLOGY

A. Method

For conducting this study, we utilized three datasets: geomagnetic storm data including planetary K-index (Kp) and disturbance storm time (Dst) indices, GPS TEC measurements from GNSS receiver equipment, and IGS TEC data. The IGS network of GPS receivers has been established, enabling consistent and regular observations. We focused on analyzing disruptions in the GPS delay time during severe (G4) geomagnetic storm that occurred on March 24, 2023, and April 24, 2023. The Space Weather Prediction Center (SWPC) reported the observation on severe geomagnetic storms in solar cycle 25. This event marked a significant geomagnetic storm in six years. Our investigation focused on analyzing GPS TEC data collected from a multi GNSS receiver station situated at low latitudes in Chumphon, Thailand. This specific location, known as the KMITL Chumphon station. The IGS TEC is collected by IGS Organization. This service, widely recognized as the International GPS Service (IGS), provides data from more than 500 stations all over the world. GPS data acquired from IGS centers are available in a Receiver Independent Exchange Format (RINEX) format. We collected all data and calculated GPS delay time during the period of the intense G4 geomagnetic storm, specifically from March 21, 2023, to March 29, 2023. The research methodology can be summarized as follows: Frist, we had data on severe geomagnetic storm event and categorized them based on physical indicators, including Kp and Dst indices. Second, IGS TEC data were obtained from IGS station at CPNM00THA, Chumphon, Thailand (10.725°N, 99.374°E). Then, GPS TEC raw data as RINEX files were received from GNSS receiver at KMITL Chumphon station, Thailand, (10.724°N, 99.375°E). Subsequently, we used the RINEX data to determine both of Slant Total Electron Content (STEC) and Vertical Total Electron Content (VTEC). Next, we calculated the GPS delay time. In conclusion, we conducted data analysis and provided a concise summary of our study findings.

B. Geomagnetic Storm

During the 25th solar cycle, the increase in solar activity and disturbances in the geomagnetic field resulted in the most severe geomagnetic storm in nearly six years. To facilitate data comparisons, a reference day was identified based on solar and geomagnetic conditions. Geomagnetic storm data were collected for the periods from March 21 to March 29, 2023, and April 21 to April 29, 2023. For a comprehensive analysis of GPS signal behavior, data were gathered over a nine-day span, including three days before the storm and five days following it. The primary focus of the analysis was on TEC irregularities and GPS signal delays. Hourly Dst index data can be accessed at: Kyoto WDC, while Kp index data are available at: NOAA SWPC. Additionally, hourly geomagnetic storm data for March 2023 can be retrieved from the IZMIRAN database at: IZMIRAN. The average intensity of the geomagnetic event was analyzed at hourly intervals using the Kp index as a reference.

C. GPS Data

The BG2 receiver is capable of receiving GPS satellite data at the KMITL station in Chumphon Province. Data from the THCP station (10.724°N, 99.375°E), THBK station (13.729°N, 100.775°E), and THCM station (18.771°N, 98.978°E) were analyzed for various types of observations. These include phase measurements for both L1 and L2 frequencies, as well as pseudo-range measurements using the C/A code on L1 (C1) and additional pseudo-range data on both L1 and L2 frequencies using the P code, labeled as P1 and P2, respectively. For this study, the focus was on observing and analyzing the signal quality and phase measurements on the L1 and L2 frequencies of GPS satellites. The data were sampled every 30 seconds. TEC values were derived from the slant path between the GPS satellite and the BG2 receiver, known as Slant Total Electron Content (STEC). The calculations for both L1 and L2 GPS frequencies were performed using the method and formula developed by Klobuchar (1996), with the resulting STEC values serving as variables for computing Vertical Total Electron Content (VTEC).

D. STEC

Each GPS satellite broadcasts signals at two distinct frequencies: f1 (1575.42 MHz) and f2 (1227.60 MHz). The receiver captures signals from 4 to 12 satellites, which are then used to STEC values. STEC, representing the electron content along the path from the satellite to the BG2s receiver, is calculated by determining the differences between P1 and P2 pseudo-ranges, as well as L1 and L2 phase differences, using Eq. (1) (Blewitt, 1990, pp. 199-202; Kenpankho et al., 2011, pp. 365-370; Keokhumcheng and Kenpankho, 2025, pp. 4245-4259).

$$\mathrm{STEC} = \frac{2(f_1 f_2)^2}{k(f_1^2 - f_2^2)}(L_1\lambda_1 - L_2\lambda_2) \quad (1)$$

where k is the related to the bending of signals due to ionospheric effects, 80.62 (m^3/s). λ_1 and λ_2 are the wavelengths with f_1 and f_2.

E. VTEC

VTEC refers to the TEC in a vertical orientation within a cross-sectional area of one square meter (Goodwin et al., 1995, pp. 1723-1732). It represents the TEC value at the point where the slant STEC intersects the ionosphere (Brunini et al., 2004, pp. 415-429). Therefore, VTEC can be considered equivalent to TEC, measured in electrons per square meter, and can be computed using the equation presented by Ma & Maruyama (2003, pp. 2083-2093), Kenpankho et al. (2011, p. 365-370), and Keokhumcheng and Kenpankho (2025, pp. 4245-4259) in Eq. (2).

$$\mathrm{VTEC} = \mathrm{STEC} \times \cos\chi \quad (2)$$

The zenith angle is defined as the angle measured from the vertical direction and is represented as χ.

$$\chi = \arcsin\left(\frac{R_E \cos\alpha}{R_E + h}\right) \quad (3)$$

where R_E is the radius of the Earth (6378 km). h is the altitude of the ionosphere layer (450 km).

F. GPS Delay Time

The GPS signal delay is calculated based on the electron density along the signal's propagation path and the corresponding carrier frequencies as

$$\Delta t = \frac{A}{cf^2} TEC \tag{4}$$

where A is the value of the refractive index of the medium.

$$\mathrm{A} = \frac{e^2}{8\pi^2 m\varepsilon_0} \tag{5}$$

where e is the electric charge (1.60217 x 10^{-19} C). m is the electron mass (9.109384 x 10^{-31} kg). ε_0 is the permittivity of free space (8.85419 x 10^{-12} F/m). A is 40.35.

$$\Delta t = \frac{1.34361\times10^{-7}}{f^2} TEC \tag{6}$$

GPS satellite signals are transmitted at f_1 = 1575.42 MHz and f_2 = 1227.60 MHz, which are defined as the primary frequencies for GPS communication.

$$\frac{1}{f^2} = \frac{1}{f_2^2} - \frac{1}{f_1^2} = \frac{f_1^2 - f_2^2}{f_1^2 f_2^2} = 2.6066\times10^{-19} \tag{7}$$

$$\Delta t = \frac{1.34361\times10^{-7}}{2.6066\times10^{-19}} TEC \tag{8}$$

$$\Delta t = 3.5023\times10^{-26} TEC \tag{9}$$

III. RESULTS

The analysis of GPS signal time delay for each event revealed significant variations influenced by geomagnetic activity. During intense geomagnetic storms, particularly on March 24, 2023 (Dst = -163 nT, Kp = 8) and April 24, 2023 (Dst = -213 nT, Kp = 8), the GPS signal delay times increased considerably, corresponding to fluctuations in TEC as follows.

A. GPS signal delay in Thailand event on March 24, 2023

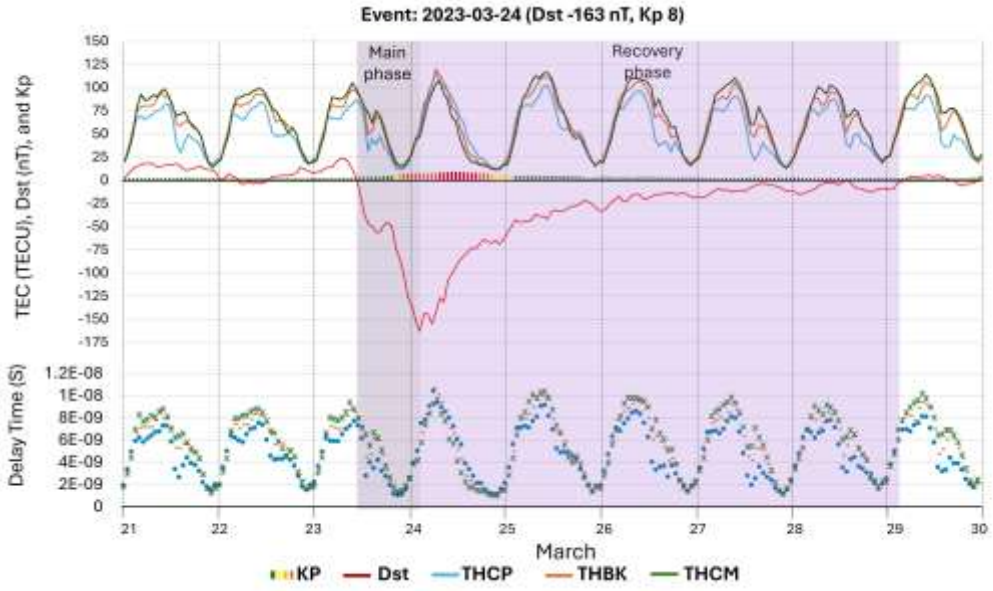

Figure 1: Analysis of the G4 Geomagnetic Storm (Dst = -163 nT, Kp = 8) on TEC and GPS signal delay in Thailand event on March 24, 2023.

This graph in Figure 1 presents an analysis of TEC, the Dst index, the Kp index, and GPS signal delay time during the geomagnetic storm event on March 24, 2023. Classified as a strong geomagnetic storm (Dst = -163 nT, Kp = 8), this event significantly impacted ionospheric conditions and GNSS signal propagation. The x-axis represents the time period from March 21 to March 29, 2023, covering the pre-storm, storm, and post-storm phases. The event is divided into two key phases: the main phase (March 24), where a significant geomagnetic disturbance occurred, and the recovery phase (March 25-29), during which the ionosphere gradually returned to normal conditions. The left y-axis displays TEC values from three GNSS stations THCP (Chumphon, blue line), THBK (Bangkok, orange line), and THCM (Chiang Mai, green line) along with the Dst index (red line), which represents global geomagnetic activity, showing a sharp drop to -163 nT on March 24, indicating a strong storm. The Kp index reflects the intensity of the storm, reaching Kp 8, signifying severe geomagnetic activity. The right y-axis illustrates GPS signal delay times (in seconds), with the lower part of the graph showing delay variations for the three GNSS stations. The delay times increased significantly during the storm, peaking on March 24, and gradually decreased as the ionosphere recovered. The TEC values exhibit daily variations, with peaks during the daytime and lower values at night. Before the storm, TEC shows a sharp increase, followed by significant fluctuations during and after the event. The Dst index reveals a negative spike at -163 nT, marking the onset of the geomagnetic storm, which corresponds to the most significant TEC disturbances and GPS signal delays. GPS signal delays fluctuate daily, closely aligning with TEC variations, and are more pronounced at lower latitudes at stations THCP (10.43 ns) and THBK (10.70 ns), where ionospheric disturbances are stronger. Overall, this graph highlights the substantial impact of geomagnetic storms on TEC and GPS signal delays, with the March 24, 2023, event causing significant ionospheric disturbances, as evidenced by a sharp drop in Dst (-163 nT), a high Kp index (8), and noticeable fluctuations in TEC and GPS delays at all three stations. These findings emphasize the strong influence of geomagnetic storms on GNSS-based applications, particularly in low-latitude regions like Thailand, where ionospheric disturbances tend to be more severe.

B. GPS signal delay in Thailand event on April 24, 2023

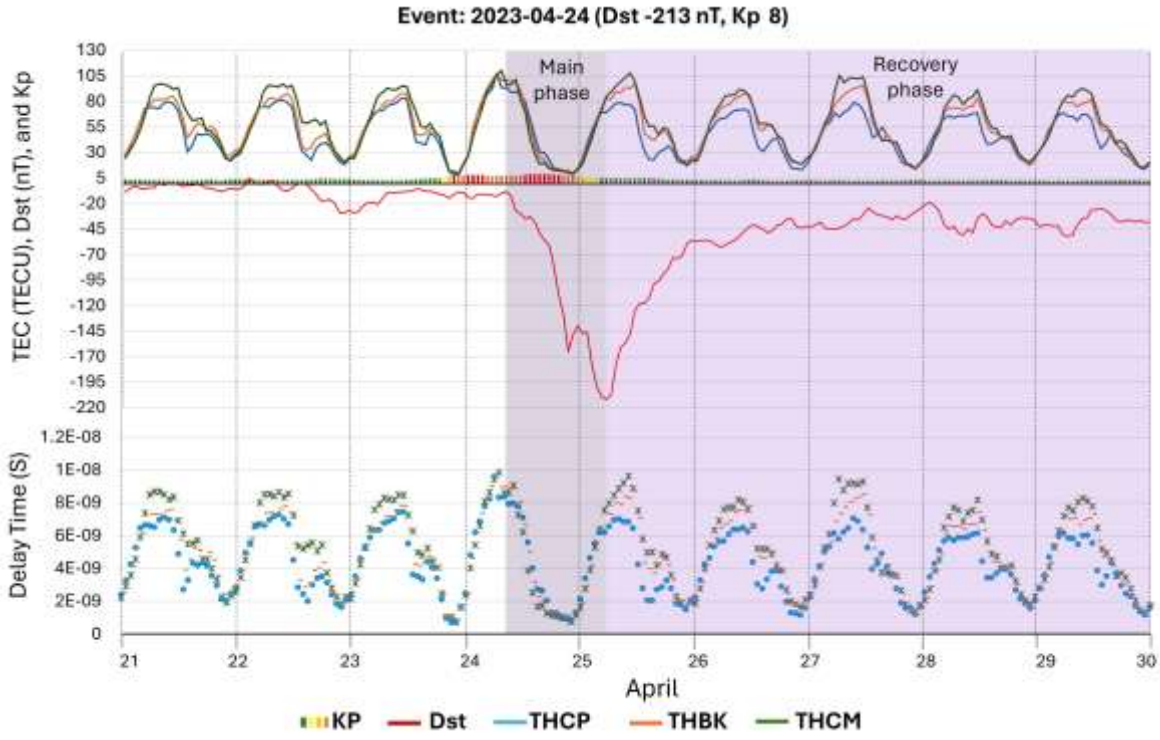

Figure 2: Analysis of the G4 Geomagnetic Storm (Dst = -213 nT, Kp = 8) on TEC and GPS signal delay in Thailand event on April 24, 2023.

This graph in Figure 2 illustrates the analysis of TEC, the Dst index, the Kp index, and GPS signal delay time during the geomagnetic storm event on April 24, 2023. Classified as a strong geomagnetic storm (Dst = -213 nT, Kp = 8), this event significantly impacted ionospheric conditions and GNSS signal propagation. The x-axis represents the time period from April 21 to April 29, 2023, covering the pre-storm, storm, and post-storm phases. The storm is divided into two key phases: the main phase (April 24), characterized by a sharp negative spike in the Dst index (-213 nT) indicating severe geomagnetic disturbance, and the recovery phase (April 25–29), during which the ionosphere gradually returned to normal conditions. The left y-axis displays TEC values from three GNSS stations THCP (Chumphon, blue line), THBK (Bangkok, orange line), and THCM (Chiang Mai, green line) alongside the Dst index (red line) and the Kp index, which reached a maximum value of Kp 8, signifying intense geomagnetic activity. The right y-axis represents GPS signal delay times (in seconds), where the lower section of the graph shows significant variations in delay times at the three GNSS stations. The delay times increased notably during the storm, peaking on April 24, before gradually decreasing as the ionosphere recovered. TEC values exhibit regular daily variations, peaking during the daytime and decreasing at night, with a sharp decrease during the main phase, indicating ionospheric disturbances. GPS signal delays show a strong correlation with TEC fluctuations, particularly at lower latitudes stations THCM (9.85 ns), THCP (9.59 ns), and THBK (9.56 ns), where ionospheric disturbances are more pronounced. Overall, this graph highlights the significant impact of the April 24, 2023, geomagnetic storm on TEC and GPS signal delays, reinforcing the strong influence of geomagnetic activity on GNSS-based applications, especially in low-latitude regions like Thailand, where ionospheric effects are more intense.

IV. DISCUSSION

The results of this study indicate that TEC values increase during geomagnetic storms compared to the periods before and after the storm, a pattern that aligns with previous findings by Liu et al. (2010, pp. 795-805), Kenpankho et al. (2011, pp. 365-370), Ratnam et al. (2011, pp. 1-6), Kenpankho et al. (2013, pp. 1820-1826), Helmboldt et al. (2015, pp. 387-402), Ansaria et al. (2019, pp. 248-258), Sedeek (2020, pp. 1-15), Zhang et al. (2021, pp. 1535-1545), and Zhbankov et al. (2022, pp. 194-201). Additionally, the impact of geomagnetic storms on TEC variations is consistent with observations by Maggiolo et al. (2017, pp. 11,109-11,127), Saito et al. (2017, pp. 1937-1947), Zhang et al. (2018, pp. 1-15), Pan and Guo (2018, pp. 1-17), Zhang et al. (2020, pp. 1-16), Zhu et al. (2020, pp. 1-14), Sedeek (2020, pp. 1-15), Zhang et al. (2021, pp. 1535-1545), and Kenpankho et al. (2021, pp. 2152-2159), all of whom reported significant TEC fluctuations associated with geomagnetic disturbances. Furthermore, the observed TEC variations closely follow the trends described by Keokhumcheng and Kenpankho (2025, pp. 4245-4259), who demonstrated that TEC values exhibit substantial fluctuations in response to geomagnetic activity, particularly in low-latitude regions. The findings from this study confirm that geomagnetic storms contribute to significant ionospheric disturbances, leading to increased GPS signal delays, further supporting the notion that TEC variations play a crucial role in affecting GNSS-based applications, particularly in low-latitude regions like Thailand, where ionospheric effects tend to be more pronounced. These results underscore the necessity of continuous ionospheric monitoring and the development of enhanced models to mitigate the adverse impacts of geomagnetic storms on satellite-based navigation and communication systems.

V. CONCLUSION

This study confirms that GPS signal delay increases significantly during intense geomagnetic storms, particularly in low-latitude regions like Chumphon, Bangkok, and Chiang Mai, Thailand. The results show that on March 24, 2023, and April 24, 2023, the GPS signal delay was notably higher compared to quiet days, aligning with the findings of Kenpankho et al. (2021, pp. 2152-2159), who analyzed GPS receiver delay in the same region from 2004 to 2019 and reported that delays were consistently higher on disturbed days. While GPS delay on quiet days ranged between 4.25 and 5.75 ns, it increased to 5.25-6.85 ns during geomagnetic storms. In this study, during the March 24, 2023, storm, the delay peaked at 0.1 ns and dropped between 38 and 40 ns, before gradually returning to normal levels after the storm, with a maximum of 0.25-0.3 ns and a minimum of 49-50 ns. Furthermore, these findings are consistent with the research of Keokhumcheng and Kenpankho (2025, pp. 4245-4259), which emphasized the significant impact of TEC variations in the ionosphere over low-latitude regions such as Chumphon Province. Overall, this study reinforces the strong correlation between geomagnetic activity, TEC fluctuations, and GPS signal delay, highlighting the need for continuous monitoring and improved ionospheric models to enhance GNSS accuracy, particularly in low-latitude regions prone to ionospheric disturbances.

ACKNOWLEDGEMENT

This research was completed with the cooperation of multiple organizations. We would like to express our gratitude to the Institute of Geology and Geophysics, Chinese Academy of Sciences (IGGCAS), and the Earthquake Observation Division (EOD), Thai Meteorological Department (TMD), for their support in providing the BG2 GNSS receiver and for their valuable guidance in this study. We also appreciate IRI and IGS for providing TEC data used for TEC validation, as well as the Space Weather Prediction Center (SWPC) of the National Oceanic and Atmospheric Administration (NOAA) for geomagnetic storm activity data. We would like to express our gratitude to IZMIRAN for supplying the hourly geomagnetic storm data along with the Kp indices. Additionally, we appreciate the World Data Center (WDC) for Geomagnetism in Kyoto, Japan, for providing the

Dst index data. Lastly, we extend our sincere appreciation to the Space Satellite Study Laboratory (SSS Lab), School of Industrial Education and Technology (SIET), King Mongkut's Institute of Technology Ladkrabang (KMITL), for their support in providing equipment and facilities for data collection.

REFERENCES

Ansari, K., Park, K.-D., & Kubo, N. (2019). Linear time-series modeling of the GNSS based TEC variations over Southwest Japan during 2011–2018 and comparison against ARMA and GIM models. *Acta Astronautica, 165*, 248-258.

Blewitt, G. (1990). An automatic editing algorithm for GPS data. *Geophysical Research Letters, 17*(3), 199-202.

Brunini, C., Meza, A., Azpilicueta, F., Van Zele, M. A., Gende, M., & Díaz, A. (2004). A new ionosphere monitoring technology based on GPS. *Astrophysics and Space Science, 290*, 415-429.

Chernyshov, A. A., Miloch, W. J., Jin, Y., & Zakharov, V. I. (2020). Relationship between TEC jumps and auroral substorm in the high-latitude ionosphere. *Scientific Reports, 10*(1), 1-13.

Chinmaya, N., Tsai, L. C., Su, S. Y., & Galkin, I. A. (2016). Peculiar features of the low-latitude and mid-latitude ionospheric response to the St. Patrick's Day geomagnetic storm of 17 March 2015. *Journal of Geophysical Research: Space Physics, 121*(8), 7941-7960.

Coster, A. J., Gaposchkin, E. M., & Thornton, L. E. (1992). Real-time ionospheric monitoring system using GPS. *Navigation, 39*(2), 191-204.

Goodwin, G. L., Silby, J. H., Lynn, K. J. W., Breed, A. M., & Essex, E. A. (1995). GPS satellite measurements: Ionospheric slab thickness and total electron content. *Journal of Atmospheric and Terrestrial Physics, 57*(14), 1723-1732.

Helmboldt, J. F., Kassim, N. E., & Teare, S. W. (2015). Observations of the ionospheric impact of M-class solar flares on local and hemispheric scales. *Earth and Space Science, 2*(10), 387-402.

Hofmann-Wellenhof, B., Lichtenegger, H., & Collins, J. (1992). *GPS -Global positioning system: Theory and practice* (4th ed.). Springer -Verlag wien.

Jenan, R., Dammalage, T. L., & Panda, S. K. (2021). Ionospheric total electron content response to September-2017 geomagnetic storm and December-2019 annular solar eclipse over Sri Lankan region. *Acta Astronautica, 180*, 575-587.

Kenpankho, P., Chaichana, A., Trachu, K., Supnithi, P., & Hozumi, K. (2021). Real-time GPS receiver bias estimation. *Advances in Space Research, 68*(5), 2152-2159.

Kenpankho, P., Supnithi, P., & Nagatsuma, T. (2013). Comparison of observed TEC values with IRI-2007 TEC and IRI-2007 TEC with optional foF2 measurements predictions at an equatorial region, Chumphon, Thailand. *Advances in Space Research, 52*(10), 1820-1826.

Kenpankho, P., Watthanasangmechai, K., Supnithi, P., Tsugawa, T., & Maruyama, T. (2011). Comparison of GPS TEC measurements with IRI TEC prediction at the equatorial latitude station, Chumphon, Thailand. *Earth, Planets and Space, 63*, 365-370.

Keokhumcheng, T., & Kenpankho, P. (2025). The study of total electron content on ionosphere by using single frequency GPS receiver. *Advances in Space Research, 75*(5), 4245-4259.

Klobuchar, J. A. (1986). Design and Characteristics of the GPS ionospheric time delay algorithm for single frequency users. Proceedings of the PLANS-86 conference, 280-286, New York, Institute of Electrical and Electronic Engineers, Las Vegas, NV.

Kumar, K. V., Maurya, A. K., Kumar, S., & Singh, R. (2016). 22 July 2009 total solar eclipse induced gravity waves in ionosphere as inferred from GPS observations over EIA. *Advances in Space Research, 58*(9), 1755-1762.

Liu, J., Zhao, B., & Liu, L. (2010). Time delay and duration of ionospheric total electron content responses to geomagnetic disturbances. *Annales Geophysicae, 28*(3), 795-805.

Ma, G., & Maruyama, T. (2003). Derivation of TEC and estimation of instrumental biases from GEONET in Japan. *Annales Geophysicae, 21*(10), 2083-2093.

Maggiolo, R., Hamrin, M., De Keyser, J., Pitkänen, T., Cessateur, G., Gunell, H., & Maes, L. (2017). The delayed time response of geomagnetic activity to the solar wind. *Journal of Geophysical Research: Space Physics, 122*(11), 11,109-11,127.

Marini-Pereira, L., Lourenço, L. F. D., Sousasantos, J., Moraes, A. O., & Pullen, S. (2020). Regional ionospheric delay mapping for low-latitude environments. *Radio Science, 55*(12), 1-16.

Pan, L., & Guo, F. (2018). Real-time tropospheric delay retrieval with GPS, GLONASS, Galileo and BDS data. *Scientific Reports, 8*(1), 1-17.

Pi, X., Mannucci, A. J., Lindqwister, U. J., & Ho, C. M. (1997). Monitoring of global ionospheric irregularities using the worldwide GPS network. *Geophysical Research Letters, 24*(18), 2283-2286.

Ratnam, D. V., Sarma, A. D., Srinivas, V. S., & Sreelatha, P. (2011). Performance evaluation of selected ionospheric delay models during geomagnetic storm conditions in low-latitude region. *Radio Science, 46*(03), 1-6.

Reddy, C. A. (1986). The equatorial ionosphere. *Indian Journal of Radio & Space Physics, 15*(5&6), 247-263.

Reddybattula, K. D., Panda, S. K., Ansari, K., & Peddi, V. S. R. (2019). Analysis of ionospheric TEC from GPS, GIM and global ionosphere models during moderate, strong, and extreme geomagnetic storms over Indian region. *Acta Astronautica, 161*, 283-292.

Saito, S., Sunda, S., Lee, J., Pullen, S., Supriadi, S., Yoshihara, T., Terkildsen, M., Lecat, F., & ICAO APANPIRG Ionospheric Studies Task Force. (2017). Ionospheric delay gradient model for GBAS in the Asia-Pacific region. *GPS Solutions, 21*, 1937-1947.

Sedeek, A. (2020). Ionosphere delay remote sensing during geomagnetic storms over Egypt using GPS phase observations. *Arabian Journal of Geosciences, 13*(811), 1-15.

Serafimov, K. B., Arshinkov, I. S., Bochev, A. Z., Petrunova, M. H., Stanev, G. A., & Chapkanov, S. K. (1982). A measuring equipment for electric and magnetic fields in the range of the ionosphere-Magnetosphere plasma mounted aboard the “Intercosmos-Bulgaria 1300” satellite. *Acta Astronautica, 9*(6-7), 397-399.

Skone, S., & de Jong, M. (2000). The impact of geomagnetic substorms on GPS receiver performance. *Earth, Planets and Space, 52*, 1067-1071.

Verkhoglyadova, O., Maus, N., & Meng, X. (2021). Classification of high density regions in global ionospheric maps with neural networks. *Earth and Space Science, 8*(7), 1-12.

Walker, J. K. (1989). Spherical cap harmonic modelling of high latitude magnetic activity and equivalent sources with sparse observations. *Journal of Atmospheric and Terrestrial Physics, 51*(2), 67-80.

Zhang, Z., Guo, F., & Zhang, X. (2018). The effects of higher-order ionospheric terms on GPS tropospheric delay and gradient estimates. *Remote Sensing, 10*(10), 1-15.

Zhang, S., He, L., & Wu, L. (2020a). Statistical study of loss of GPS signals caused by severe and great geomagnetic storms. *Journal of Geophysical Research: Space Physics, 125*(9), 1-16.

Zhang, Y., Wu, Z., Feng, J., Xu, T., Deng, Z., & Zhen, W. (2020b). Statistical study of the time delay of ionospheric TEC storms to geomagnetic storms in Taoyuan, Taiwan. *Advances in Space Research, 65*(1), 86-94.

Zhang, Y., Wu, Z., Feng, J., Xu, T., Deng, Z., Ou, M., & Xiong, W. (2021). Time delay of ionospheric TEC storms to geomagnetic storms and pre-storm disturbance events in East Asia. *Advances in Space Research, 67*(5), 1535-1545.

Zhbankov, G. A., Danilkin, N. P., & Maltseva, O. A. (2022). Influence of the ionosphere on the accuracy of the satellite navigation system. *Acta Astronautica, 190*, 194-201.

Zhu, F., Zhang, H., Huang, L., Li, X., & Feng, P. (2020). Research on absolute calibration of GNSS receiver delay through clock-steering characterization. *Sensors, 20*(21), 1-14.

THE CHARACTERISTICS OF TOTAL ELECTRON CONTENT DISTURBANCES AT LOW LATITUDES DURING SEVERE GEOMAGNETIC STORM EVENTS ON MARCH 24 AND APRIL 24, 2023

Chollada Pansong[1]*, Samatchaya Maichuen[2], and Pattawut Wongsak[2]
E-mail: chollada_p@rmutt.ac.th[1*], 67036099@kmitl.ac.th[2], and 67036098@kmitl.ac.th[2]

Received: August 16, 2024
Revised: October 14, 2024
Accepted: November 25, 2024

ABSTRACT

This study investigated the Total Electron Content (TEC) characteristics at two different low latitudes and three different TEC sources during the severe geomagnetic storms, focusing on the events of March 24, 2023, and April 24, 2023. TEC data were collected from GNSS receivers in Chumphon (THCP station: 10.724°N, 99.375°E), and Bangkok (THBK station: 13.729°N, 100.780°E), Thailand, using three sources: GNSS satellite receivers, the International GNSS Service (IGS), and the International Reference Ionosphere (IRI). GPS TEC, IGS TEC, and IRI TEC values were compared among them. The correlation coefficient between geomagnetic storm intensity and ionospheric TEC disturbances was analyzed. The results show that geomagnetic storm levels strongly influence ionospheric TEC disturbances. TEC values typically increase during storms and return to normal within a few days. During the storm events, TEC increased up to 75% over Chumphon and 10-35% over Bangkok. The strong geomagnetic storms exhibited positive correlations with higher TEC values, while quiet periods showed no significant decreases below baseline levels, indicating a negative correlation coefficient.

Keywords: Geomagnetic storm, GPS TEC, IGS TEC, IRI TEC, Low latitude

*Corresponding author E-mail: chollada_p@rmutt.ac.th
[1*]Department of Technical Education, Faculty of Technical Education, Rajamangala University of Technology Thanyaburi, Pathum Thani, 12110 Thailand
[2]Department of Engineering Education, School of Industrial Education and Technology, King Mongkut's Institute of Technology Ladkrabang, Bangkok, 10520 Thailand

I. INTRODUCTION

The Global Navigation Satellite System (GNSS) provides a reliable reference and a novel approach for sensing natural dynamics. One of its components, the Global Positioning System (GPS), relies on signal quality affected by electron diffusion in the ionosphere (Chernyshov et al., 2020, p. 1). The ionosphere, as a propagation medium, slows signal transmission depending on plasma density. Disturbances in the ionosphere negatively impact GPS accuracy and reliability, with free electrons influencing signal phase and amplitude. The ionosphere's Total Electron Content (TEC) affects the group delay and phase advance of GPS signals, with higher TEC values causing a more significant signal impact. Irregular plasma density leads to wave distortion, resulting in inaccurate parameter estimation or temporary signal interruptions (slips). Ionospheric anomalies arise from disturbances in Earth's space environment caused by solar and geophysical factors. Influences such as the Interplanetary Magnetic Field (IMF), solar wind, geomagnetic storms, and sub-storms contribute to near-Earth plasma conditions and their relation to solar activity (Hofmann-Wellenhof et al., 1992, pp. 90-97; Pi et al., 1997, p. 2283; Skone & de Jong, 2000, p. 1067; Chernyshov et al., 2020, p. 1; Tsurutani et al., 2020).

Positive ionospheric storms are linked to enhanced electron density caused by thermospheric winds, compositional changes, ionization, and electric field transport. In contrast, negative storms primarily result from compositional changes in the ionosphere (Nayak et al., 2016, pp. 7941-7960; Reddybattula et al., 2019, p. 283; Serafimov et al., 1982, pp. 397-399). TEC disturbances caused by geomagnetic storms vary with latitude. At low latitudes, electromagnetic fields strongly influence TEC over the magnetic equator, leading to increased electrical conductivity (Li et al., 2019, p. 9380). During storms, ionospheric currents and energetic particles release heat energy, elevating and redistributing atmospheric density, which increases drag on low-Earth orbit satellites. The ionosphere is classified into high-, mid-, low-latitude, and equatorial regions. Low-latitude and equatorial regions (±20° of the geomagnetic equator) exhibit high electron density and complex variations caused by phenomena such as the Equatorial Ionization Anomaly (EIA) and Equatorial Electrojet (EEJ). Research on these regions is vital for understanding ionospheric morphology and improving modeling techniques (Jenan et al., 2021, pp. 575-587; Kumar et al., 2016, pp. 1755-1762; Reddy, 1986, pp. 247-263).

Previous studies include Kenpankho et al. (2011, pp. 365-370), who compared GPS TEC and IRI predictions at Chumphon; Rao et al. (2013, pp. 1-6), who studied TEC variability along 73°E; and Nava et al. (2016, pp. 3421-3438), who analyzed mid- and low-latitude ionospheric responses to the 2015 St. Patrick's Day storm. Zhou et al. (2016, pp. 9146-9163) investigated ionospheric storm effects during the March 2015 event, while Chen et al. (2017, pp. 3632-3639) examined geomagnetic activity's influence on TEC using different analytical methods. Reddybattula et al. (2019, p. 283) analyzed TEC during various geomagnetic storm intensities in India, and de Paula et al. (2019, pp. 1-15) studied ionospheric irregularities over Brazil during the September 2017 storm. Additional research includes Dugassa et al. (2019, pp. 1161-1180), who examined TEC gradients and irregularities; Mansilla (2019, pp. 26-36), who studied TEC behavior in polar regions during intense storms; and Ali et al. (2021, pp. 4857-4871), who analyzed transient TEC variations at low latitudes. Ratovsky et al. (2022, pp. 1-15) linked extreme ionospheric events to geomagnetic activity, while Klimenko et al. (2017, pp. 923-938) reported on similarities and differences in morphology and mechanisms of the foF2 and TEC disturbances during the geomagnetic storms on September 26-30, 2011. Machine learning-based TEC modeling during storms was explored by Adolfs et al. (2022, pp. 1-17).

Finally, Bojilova and Mukhtarov (2023, pp. 1-23) analyzed global and regional ionospheric responses during the February 2022 storms. After reviewing relevant studies, we designed research to investigate, analyze, and compare low-latitude TEC disturbances over Bangkok and Chumphon, Thailand, during the severe geomagnetic storms of March 24, 2023, and April 24, 2023. TEC data were collected from three sources: GPS, the International GNSS Service (IGS), and the International Reference Ionosphere (IRI), to conduct a comprehensive analysis of these disturbances. Chen et al. (2017, pp. 3632-3639) examined the impact of geomagnetic activity on TEC data, comparing the Spectral Whitening Method (SWM) and the 28-day Running Median Centered (RMC) technique. They found that RMC overestimated disturbances by 5–20% during geomagnetic storms and up to 35% during quiet conditions compared to SWM. Similarly, Nava et al. (2016, pp. 3421-3438) analyzed ionospheric responses at mid- and low latitudes during the 2015 St. Patrick's Day storm. In the Asian sector, they compared mid-latitude stations Wuhan (Northern Hemisphere) and Yar2 (Southern Hemisphere) with the low-latitude station Cusv (Northern Hemisphere). They observed significant TEC decreases at mid-latitudes for several days post-storm but found TEC increased at low latitudes on the storm day with no subsequent decline. These results highlight the concentration of ionization at low latitudes near the equator following storms, while mid-latitudes experience significant reductions.

These results highlight the concentration of ionization at low latitudes near the equator following storms, while mid-latitudes experience significant reductions. According to results, based on these findings, our research aims to provide detailed insights into TEC disturbances at low latitudes, particularly in Bangkok and Chumphon, by leveraging GPS, IGS, and IRI data during the severe geomagnetic storms of March and April 2023 with the contribution of the understanding ionospheric behavior in equatorial regions and improving TEC disturbance modeling.

II. METHODOLOGY

Our research focused on TEC disturbances during two severe geomagnetic storms analyzed on March 24, 2023, and April 24, 2023, reported by the Space Weather Prediction Center (SWPC) as the second and third G4-class storms of Solar Cycle 25. These events marked the strongest geomagnetic storms in nearly six years. TEC data were analyzed from low-latitude GNSS receiver stations: THBK (13.729°N, 100.780°E) at King Mongkut's Institute of Technology Ladkrabang (KMITL) in Bangkok and THCP (10.724°N, 99.375°E) in Chumphon, Thailand. Data collection took place from March 21 to 29, 2023, and from April 20 to 28, 2023. The research methodology included the following steps:

1. Geomagnetic Storm Classification: Geomagnetic storm events were classified using the Planetarische Kennziffer (Planetary Index: Kp), Disturbance Storm Time (Dst) index, and Geomagnetic Auroral Electrojet (AE) index.

2. GNSS TEC Data Collection: GPS TEC data were extracted from Receiver Independent Exchange Format (RINEX) files obtained from GNSS receivers at THBK and THCP stations. Slant TEC (STEC) and Vertical TEC (VTEC) were calculated.

3. Supplementary TEC Data: IGS TEC data were acquired from IGS, and IRI TEC data were obtained from the International Reference Ionosphere (IRI).

4. Data Processing: The GPS TEC, IGS TEC, and IRI TEC were calculated using three-hour median values aligned with geomagnetic storm indices.

5. Data Analysis: The collected data were analyzed to evaluate TEC disturbances, and the findings were summarized.

This comprehensive approach provides insights into TEC behavior during severe geomagnetic storms at low latitudes, contributing to a better understanding of ionospheric dynamics.

A. GPS TEC Analysis

GPS TEC is derived by analyzing the delay in travel time of multi-frequency GPS signals received at GNSS stations. This involves both pseudorange and carrier phase measurements, which estimate the distance between GPS satellites and the receiver. The accuracy of these measurements depends not only on the satellite and receiver systems but also on environmental factors such as the ionosphere, troposphere, and multipath effects. The carrier phase measurements at L1 and L2 frequencies are calculated as follows.

$$L_1 = p - I_{p_1} + c(\tau^r_{p_1} - \tau^s_{p_1}) + T + \lambda_1 n_1 + \varepsilon_{L_1},$$
$$L_2 = p - I_{p_2} + c(\tau^r_{p_2} - \tau^s_{p_2}) + T + \lambda_2 n_2 + \varepsilon_{L_2}, \quad (1)$$

where L_1 and L_2 are carrier phase measured on the frequency of L_1 and L_2 respectively, p is geometrical range from satellite s to receiver r, τ^r is receiver clock error, τ^s is satellite clock error, T is a tropospheric delay, $I_{P1/2}$ are ionospheric delays in code measurement on $L_{1/2}$, $\lambda_{1/2} n_{1/2}$ are integer cycle ambiguities $\varepsilon_{P1/2}$ are multipath delays and other delays/errors in code measurement on $L_{1/2}$.

The L_1 and L_2 values for each GPS satellite are obtained from RINEX. Then, the STEC can be calculated in the next section. To map TEC measurements geographically, the thin shell model is used, representing the ionosphere as a spherical shell at a specific height (h). An elevation mapping function converts STEC measurements to VTEC values, which are then assigned to geographic locations based on the Ionospheric Pierce Point (IPP). The model assumes a shell height corresponding to the F2 peak density (hmF2) at approximately 400 km over Thailand (Kenpankho et al., 2011, p. 366). In GNSS systems like GPS, satellites transmit signals at multiple frequencies, such as f1 (1575.42 MHz) and f2 (1227.60 MHz). A GNSS receiver simultaneously receives signals from 4–12 satellites, allowing the computation of STEC values. $STEC_L$ is determined by calculating the differences between carrier phases (L1 and L2) of the two frequencies. These calculations are defined by Equations (2) (Blewitt, 1990, pp. 199–202; Kenpankho et al., 2011, p. 366).

$$\mathrm{STEC_L} = \frac{2\left(f_1 f_2\right)^2}{k\left(f_1^2 - f_2^2\right)}\left(L_1\lambda_1 - L_2\lambda_2\right), \quad (2)$$

where k, related to the ionosphere refraction, is 80.62 (m^3/s^2), λ_1, and λ_2 (λ_1 = 0.1904 m, λ_2 = 0.2444 m) are the wavelengths corresponding to f_1 and f_2, respectively.

VTEC represents the total number of electrons (in electrons per square meter; el/m²) in a vertical column with a one-square-meter cross-section (Goodwin et al., 1995, pp. 1723–1732). For GPS TEC, this refers to VTEC measured at the Ionospheric Pierce Point (IPP), accounting for the obliquity factor (Brunini et al., 2004, pp. 415–429). VTEC, in el/m², is derived from GPS STEC measurements by applying the obliquity factor, as shown in Equation (3) (Kenpankho et al., 2011, p. 366; Ma & Maruyama, 2003, p. 2084).

$$\mathrm{VTEC} = \mathrm{STEC}_L \times \cos\chi, \quad (3)$$

The zenith angle (χ) is the angle between a given location on the Earth's surface and the vertical direction pointing directly overhead. It is measured from the zenith, which is the point in the sky directly above an observer. The zenith angle (χ) is expressed from Equation (4) as

$$\chi = \arcsin\left(\frac{R_E \cos\alpha}{R_E + h}\right), \quad (4)$$

where R_E is the mean radius of the Earth, approximately 6,371 km, α is the elevation angle of the satellite, and h is the height of the ionospheric layer, which is assumed to be 400 km (Kenpankho et al., 2011, p. 366; Ma & Maruyama, 2003, p. 2084)

B. IGS TEC data

The IGS TEC, which stands for ionospheric TEC, is managed and supervised by the IGS organization. The IGS utilizes a global network of more than 515 GNSS data stations that operate continuously and provide high-quality multi-frequency data. The IGS has been recognized as an official service of the International Association of Geodesy (IAG) since 1994. It has also been a member of the Federation of Astronomical and Geophysical Data Analysis Services (FAGS) since 1996. The IGS is responsible for collecting, archiving, and distributing GPS observation data sets. Additionally, the IGS offers TEC map data, which is accessible through the File Transfer Protocol (FTP) for users to access and utilize. The IGS TEC data can be accessed through their FTP site at: https://igs.org. We selected the available IGS station located at CUUT00THA, Bangkok, Thailand (13.736°N, 100.534°E). There is also a station close to THBK, station (13.729°N, 100.780°E). The CPNM00THA, Chumphon, Thailand (10.725°N, 99.374°E) was chosen because it is located close to the THCP station (10.724°N, 99.375°E). We collected IGS TEC data for a total of nine days, starting three days before the severe geomagnetic storm occurred and continuing for five days after the severe geomagnetic storm occurred. Lastly, we analyzed the IGS TEC data during geomagnetic storm events based on the Dst, AE, and Kp indices time using the median statistic. The results of the IGS TEC data analyzed are presented in the following section.

C. IRI TEC data

The IRI is an organization established to develop an international standard for ionospheric parameters identifying. This standard is based on comprehensive data obtained from ground-based and satellite observations and it was initiated by the Committee on Space Research (COSPAR) and the International Union of Radio Science (URSI) in the late 1960s (Bilitza & Rinisch, 2008, pp. 599-609). TEC can be obtained from the IRI model, and it is referred to as IRI TEC. The IRI model is continually upgraded as new data and new modeling methods become available. This process has resulted in several milestone editions of the IRI (Bilitza, 1990, pp. 1–146; Bilitza, 2001, pp. 261-275; Bilitza & Rawer, 1996, pp. 735-772; Bilitza & Reinisch, 2008, pp. 599-609; Rawer et al., 1978a, pp. 177-181; Rawer et al., 1978b, pp. 6.1-6.10). Currently, the IRI-2020 is a new and improved empirical standard model of the ionosphere, addressing the limitations of its predecessors. The IRI-2020, the new empirical standard model of the ionosphere, is accessible at the following website: https://kauai.ccmc.gsfc.nasa.gov/instantrun/iri/. IRI TEC data were collected three days before the severe geomagnetic storm happened and five days after the severe geomagnetic storm happened, nine days in total. We input the location, date, and time to match the specific station's location and the period of the geomagnetic storm occurrence. In the final step, we analyzed the IRI TEC data, specifically focusing on the geomagnetic storm events that occurred during the designated periods according to the Dst, AE, and Kp indices. The analysis was performed using the median statistic. The results of the IRI TEC data analysis are presented in the next part.

D. Geomagnetic storm data

On March 24, 2023, the SWPC reported observing the second severe geomagnetic storm (G4) in solar cycle 25, which was the largest such event in nearly six years. The aurora was visible in more than half of the United States, reaching as far south as New Mexico, Missouri, and North Carolina. The second severe geomagnetic storm in 2023 occurred on Sunday, April 23, 2023, and continued until April 24, 2023, causing rare auroras to sparkle across Germany and France. Therefore, the geomagnetic storm data were collected for the periods of March 21-29, 2023, and April 20-28, 2023. We collected data for a total of nine days: three days before the severe geomagnetic storms occurred and five days after the severe geomagnetic storms occurred according to the TEC disturbances. The hourly equatorial Dst values can be found at https://wdc.kugi.kyoto-u.ac.jp/dst_realtime/index.html for geomagnetic storm indicators. AE index data were collected from the WDC for Geomagnetism Kyoto at https://wdc.kugi.kyoto-u.ac.jp/ae_realtime/index.html. The Kp index is a measure of geomagnetic activity on Earth, ranging from 0 to 9, with higher values indicating more significant geomagnetic disturbances and potential for brighter auroras. The Kp index geomagnetic storms were collected from the National Oceanic and Atmospheric Administration (NOAA), SWPC at the website https://www.swpc.noaa.gov/. The Kp index, which ranges from 0 to 9 in one-third increments, represents the average of the Ks indices obtained from 13 contributing geomagnetic observatories located at sub-auroral latitudes, collectively known as Kp stations.

E. Correlation coefficient

We also analyzed the correlation coefficient between geomagnetic storm levels and TEC values, including GPS TEC, IGS TEC, and IRI TEC. Correlation coefficient (r), which quantifies the linear relationship between variables x (geomagnetic storm level) and y (TEC values), and is calculated using Equation (5) (Mukaka, 2012, p. 69).

$$r = \frac{\sum_{i=1}^{n}(x_i - x)(y_i - y)}{\sqrt{\left[\sum_{i=1}^{n}(x_i - \bar{x})^2\right]\left[\sum_{i=1}^{n}(y_i - \bar{y})^2\right]}} \quad (5)$$

In this context, *r* signifies the correlation coefficient of the linear association between the variables *x* and *y*., x_i represents the geomagnetic storm scale value in a sample, $\bar{x}$ signifies the mean of the geomagnetic storm scale values, y_i indicates the TEC values in a sample, and $\bar{y}$ denotes the mean of the TEC values.

III. RESULTS

A. Geomagnetic storm levels

The results of the geomagnetic storm data analysis are plotted in Figures 1 and 2.

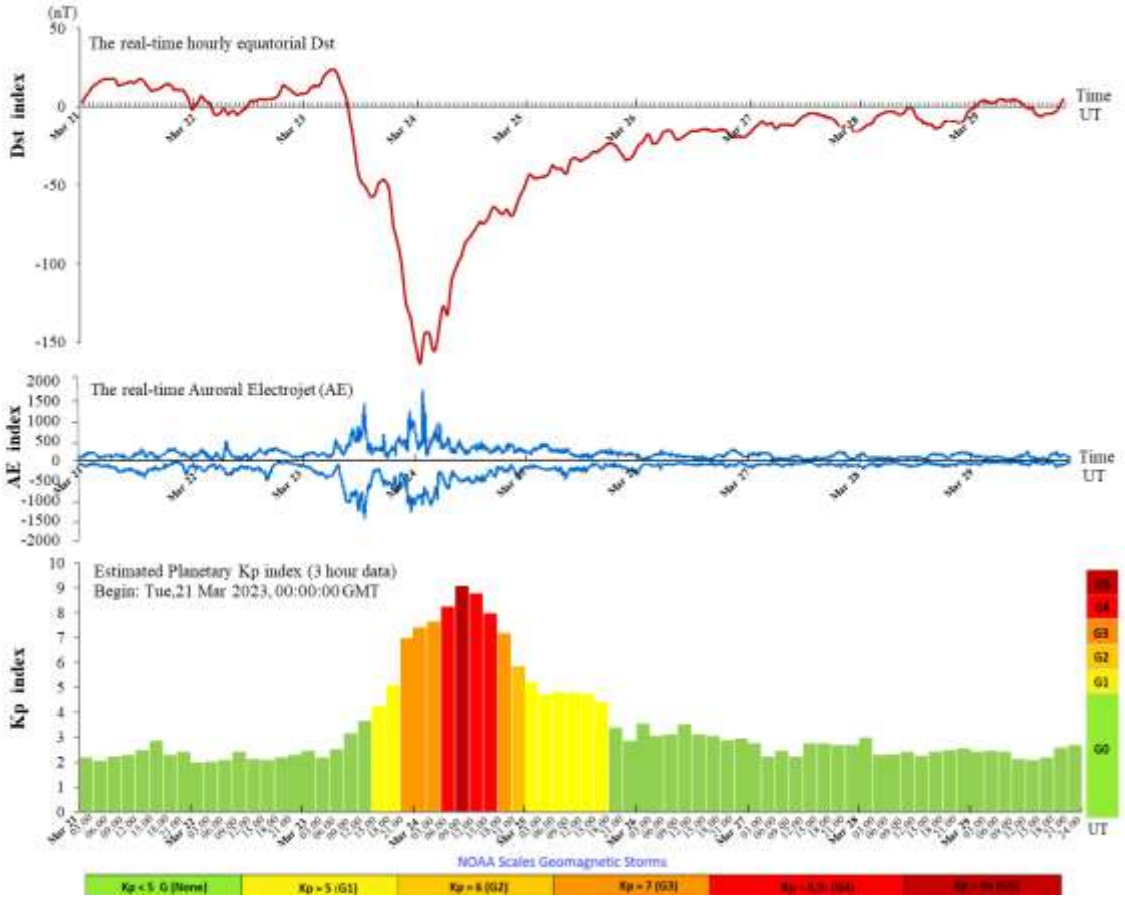

Figure 1: The Dst, AE, and Kp indices of the G4 severe geomagnetic storm that occurred from March 21-29, 2023.

Figure 1, the geomagnetic storm intensified from G1 (Kp = 5), G2 (Kp = 6), and G3 (Kp = 7) levels continuing into the late hours of March 23rd. On March 24th, the average intensity of the geomagnetic storm reached G4 level (Kp = 8,9-). Subsequently, the storm intensity decreased on March 25th and returned to normal on the following day. On March 23, 2023, solar activity was recorded at very low levels over the past 24 hours. According to SWPC's report, there were five numbered sunspots. The forecast indicated that solar activity would remain low with a slight chance of a flare on days one, two, and three following the geomagnetic storm days (24th, 25th, and 26th March). On March 28, 2023, the sun emitted a strong solar flare, which reached its peak as observed by the National Aeronautics and Space Administration (NASA)'s Solar Dynamics Observatory.

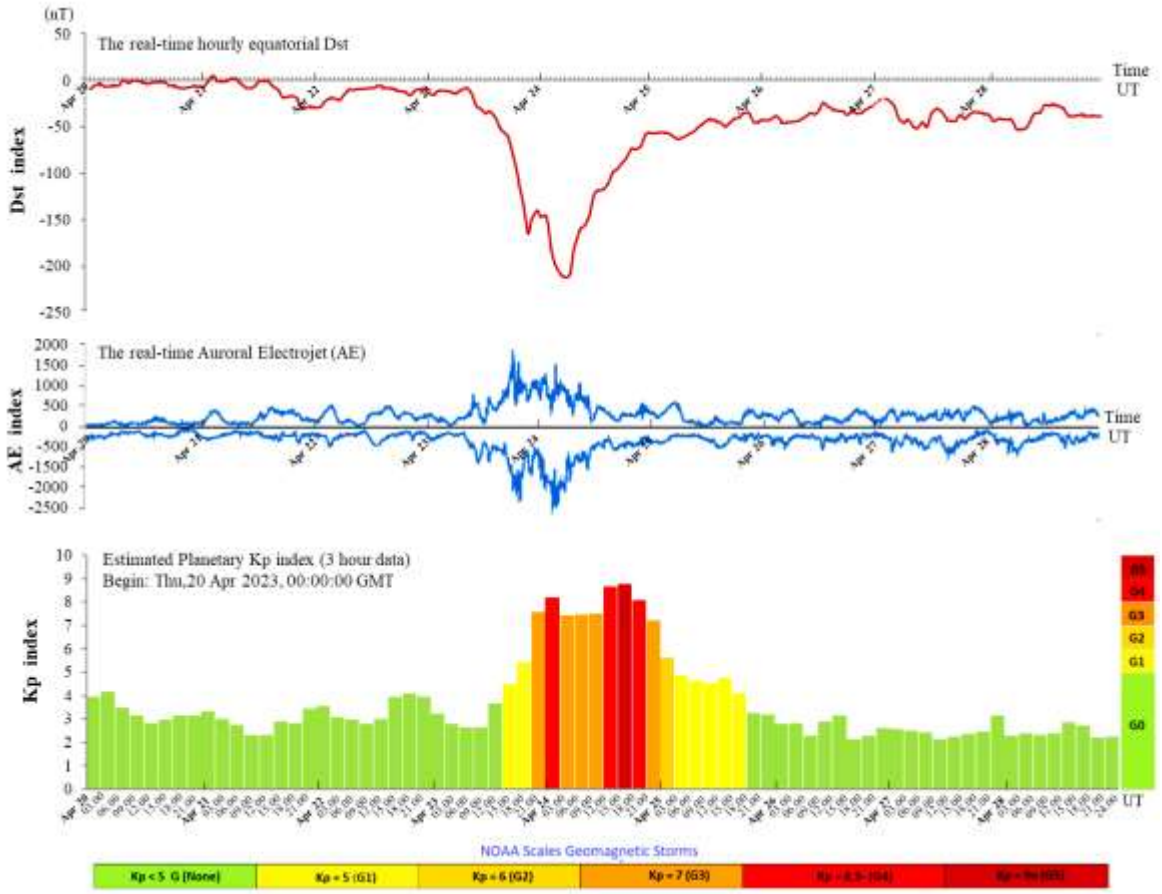

Figure 2: The Dst, AE, and Kp indices of the G4 severe geomagnetic storm that occurred from April 20-28, 2023.

Figure 2 illustrates the geomagnetic storm data collected from April 20-28, 2023. The graph revealed that the geomagnetic storm watches were in effect from April 23 to April 24, 2023. During this storm period, the storm intensified, reaching G1 (Kp = 5), G2 (Kp = 6), and G3 (Kp = 7) levels, and this continued into the late hours of April 23. On the night of April 23, the G3 period occurred and intensified further on April 24, reaching extreme storm at the G5 (Kp = 90) level. The average intensity of geomagnetic storms on April 24 was classified as a severe storm at the G4 (Kp = 8,9-). After that, the storm intensity gradually decreased on April 25 and returned to normal levels on the next day.

B. TEC disturbances during the storm time

After analyzing the data from GPS TEC, IGS TEC, and IRI TEC, we plotted the TEC data against the Dst, AE, and Kp indices as shown in Figures 3 and 4. There are GPS TEC, IGS TEC, and IRI TEC, which were observed during March 21-29, 2023, at the THBK station and during April 20-28, 2023, at the THCP station. The results indicated the notable significance of TEC anomalies during the geomagnetic storm day compared to the quiet geomagnetic stormy days, as shown in Figures 3 and 4.

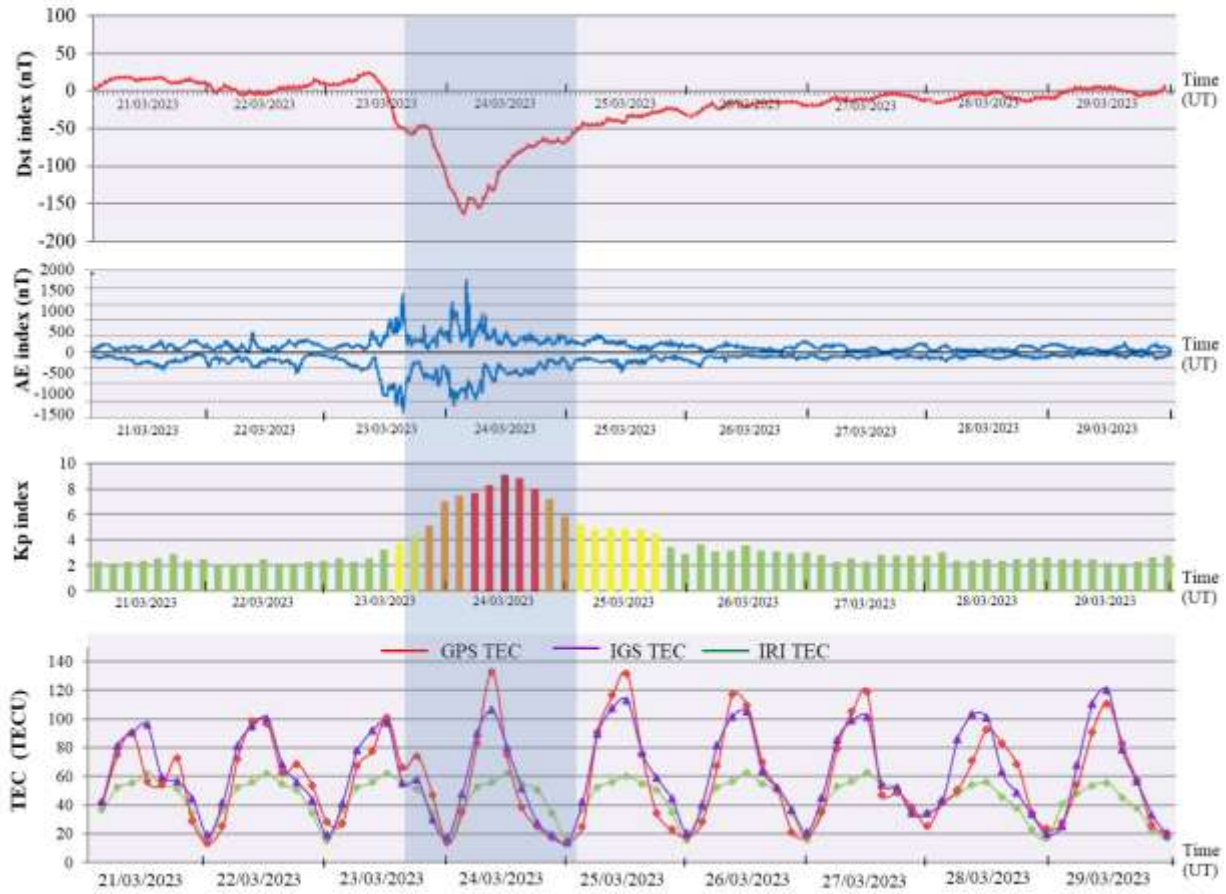

Figure 3: Anomalous TEC was observed over Bangkok, Thailand, during the period of severe geomagnetic storm from March 21-29, 2023.

Figure 3 presents a time series analysis of geomagnetic activity and TEC variations over the period from 21 to 29 March 2023. The four panels illustrate the Dst index, AE index, Kp index, and TEC values derived from GPS, IGS, and IRI models, respectively. In the first panel, the Dst index shows a pronounced drop reaching at –163 nT on 24 March 2023, indicating a strong geomagnetic storm. This sharp decrease highlights the main phase of the storm, which is also marked by the shaded region in the figure. The second panel displays the AE index, reflecting auroral electrojet activity. A significant spike occurs concurrently with the Dst minimum, confirming intense auroral activity during the storm period. In the third panel, the Kp index rises dramatically, peaking at Kp 8, which also indicates severe geomagnetic storm conditions. The elevated Kp levels persist for several hours on 24 March, aligning with the storm's peak intensity. The fourth panel illustrates TEC variations at a low-latitude station using three data sources: GPS TEC (red line), IGS TEC (purple line), and IRI TEC (green line). A substantial increase in TEC was observed on 24 March, particularly in the GPS and IGS data, with values peaking at above 120 TECU, compared to average daily peaks around 80-100 TECU during quieter days. This enhancement corresponds closely with the peak geomagnetic activity, suggesting a strong ionospheric response to the storm. The data presented that during geomagnetic storm-time activities, TEC tends to increase on the day of a severe storm that occurred on March 24, 2023. TEC remains high in the following days. Afterward, it gradually decreases back to normal levels within 2-3 days later. During the geomagnetic storm days, GPS TEC increased by approximately 10-35% compared to the 9-day average.

Figure 4: Anomalous TEC was observed over Chumphon, Thailand, during the period of severe geomagnetic storm from April 20-28, 2023.

Figure 4 compares geomagnetic storm activity and TEC variations from 20 to 28 April 2023. The data are presented in four panels: Dst index, AE index, Kp index, and TEC values from three sources: GPS, IGS, and IRI models. The shaded region highlights the period of the geomagnetic storm. In the first panel, the Dst index reaches a minimum value of –213 nT on 24 April 2023, indicating the main phase of an intense geomagnetic storm. This drop marks a strong disturbance in Earth's magnetic field. The second panel displays the AE index, representing auroral electrojet activity. A noticeable spike occurs concurrently with the Dst minimum, suggesting elevated auroral activity during the storm period. The third panel shows the Kp index, which reflects global geomagnetic activity. The Kp values peak at level 8 (G4) on 24 April, which signifies a severe geomagnetic event. Elevated Kp levels are observed from 23 to 25 April, confirming the duration and intensity of the storm. In the fourth panel, the TEC values are plotted from three sources: GPS TEC (red line), IGS TEC (purple line), and IRI TEC (green line). A significant TEC enhancement is evident on 24 April, with GPS TEC values peaking at approximately 175 TECU, much higher than the average on surrounding days. This increase corresponds with the timing of the geomagnetic storm, indicating a strong ionospheric response, particularly at low latitudes. The severe geomagnetic storm on April 24, 2023, is shown. TEC increases significantly on the day of the storm and begins to decrease the following day, gradually returning to normal

levels over the next few days. During the periods of geomagnetic storms, the GPS TEC increased by approximately 75% relative to the 9-day average.

Figures 5 and 6 present the Global Ionosphere Maps (GIMs) TEC during the severe geomagnetic storms of March 21–26, 2023, and April 20–25, 2023.

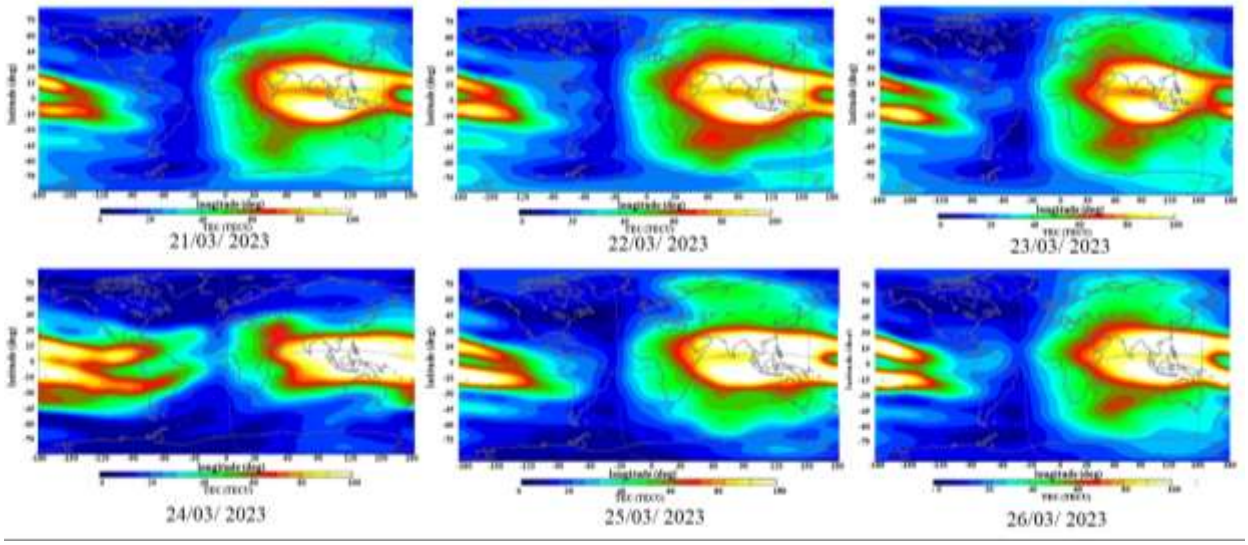

Figure 5 : The GIMs TEC during the severe geomagnetic storm period from March 21-26, 2023.

Figure 5 displays global TEC maps for six consecutive days, from 21 to 26 March 2023. Each map illustrates the spatial distribution of TEC values, measured in TEC units (TECU), with a color scale ranging from dark blue (low TEC) to red and white (high TEC). The maps focus particularly on the equatorial region, with the Southeast Asian sector, including Thailand, highlighted for reference. On 21 and 22 March, the TEC distribution appears relatively uniform with moderate intensity near the equatorial anomaly zones. There is a clear formation of EIA crests around ±15° magnetic latitude, especially over Southeast Asia. On 23 March, corresponding with a G2-class geomagnetic storm, there is a notable decrease in TEC intensity over the region, particularly around Thailand. The red and orange zones, indicating higher TEC values, are less pronounced, suggesting ionospheric disturbance. In contrast, the TEC maps for 24 and 25 March, which coincide with G4 and G2-class storms, respectively, exhibit a significant enhancement in TEC values. The equatorial anomaly intensifies, with brighter red and white zones expanding westward and eastward, indicating strong ionospheric activity likely driven by geomagnetic storm effects. By 26 March, the TEC pattern returns to a more moderate state, with the equatorial anomaly becoming more symmetric and the intensity decreasing compared to the peak seen on 24–25 March. Overall, the maps illustrate the dynamic response of the ionosphere to geomagnetic activity, particularly showing how storm intensity influences TEC variations across different longitudes and latitudes. These visualizations support the correlation analysis shown in the previous table, highlighting the significant TEC disturbances that occurred during strong geomagnetic storm events.

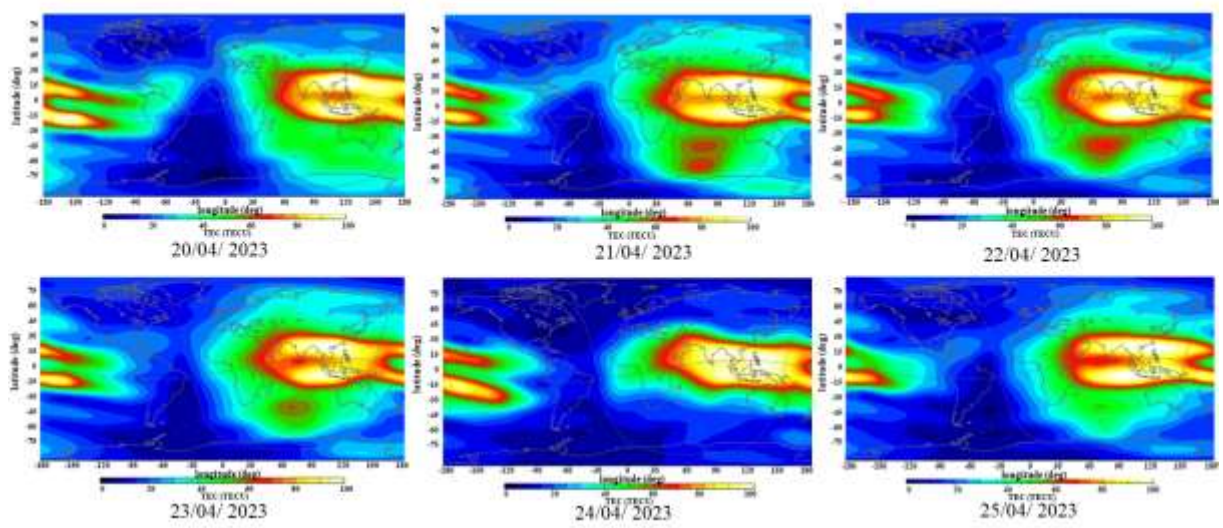

Figure 6: The GIMs TEC during the severe geomagnetic storm period from April 20-25, 2023.

Figure 6 illustrates global Total Electron Content (TEC) distributions over six consecutive days, from 20 to 25 April 2023. The TEC values, expressed in TEC units (TECU), are represented using a color scale from dark blue (low TEC) to red and white (high TEC). These maps highlight ionospheric conditions, particularly around the equatorial and low-latitude regions, with Thailand prominently marked as a reference location. On 20 April, the TEC distribution appears relatively moderate with a slight improvement around the equatorial region. Moving to 21 and 22 April, the maps show an increase in TEC intensity, particularly over Southeast Asia and the Pacific sector, indicating enhanced ionospheric activity likely associated with variations in space weather. The TEC map for 23 April, which corresponds with a G1-class geomagnetic storm, displays a further increase in TEC values, with intensified red zones and stronger Equatorial Ionization Anomaly (EIA) structures observed on both sides of the magnetic equator. The enhancement appears more asymmetric, suggesting storm-time ionospheric disturbances. On 24 April, during a G4-class geomagnetic storm, there is a pronounced increase in TEC levels, especially in the Southeast Asia–Pacific sector. The EIA becomes more intense and widespread, indicating a significant ionospheric response to strong geomagnetic activity. By 25 April, the TEC pattern shows signs of moderation, though high TEC values are still evident, particularly in regions west of the Pacific. This suggests a gradual return to quieter ionospheric conditions following the intense storm event. In summary, these maps demonstrate the temporal and spatial evolution of TEC during periods of geomagnetic activity. The strongest TEC disturbances are observed on 23 and 24 April, coinciding with the G1 and G4 storm levels, respectively. These findings align with the statistical correlation results and reinforce the impact of geomagnetic storms on ionospheric variability in low-latitude regions such as Thailand.

C. The correlation between geomagnetic storm levels and TEC disturbances

Table 1: Correlation coefficient between geomagnetic storm levels and TEC disturbances.

Correlation Coefficient (r) between TEC Disturbances and Geomagnetic Storm Levels							
THBK station, Bangkok				THCP station, Chumphon			
Storm Levels	GPS TEC	IGS TEC	IRI TEC	Storm Levels	GPS TEC	IGS TEC	IRI TEC
21/03/23 (G0)	-0.072	-0.398	-0.068	20/04/23 (G0)	-0.398	-0.304	0.344
22/03/23 (G0)	-0.035	-0.061	-0.182	21/04/23 (G0)	-0.792	-0.773	-0.518
(23/03/23) (G2)	-0.825	-0.900	-0.901	22/04/23 (G0)	-0.711	-0.819	-0.894
24/03/23 (G4)	0.482	0.595	0.955	23/04/23 (G1)	0.544	0.620	0.944
25/03/23 (G2)	0.818	0.905	0.978	24/04/23 (G4)	-0.116	-0.496	-0.118
26/03/23 (G0)	0.769	0.762	0.687	25/04/23 (G2)	0.321	0.327	0.792
(27/03/23) G0	-0.832	-0.847	-0.574	(26/04/23) G0	0.232	0.228	0.398
28/03/23 (G0)	-0.498	-0.501	-0.324	27/04/23 (G0)	-0.722	-0.744	-0.663
29/03/23 (G0)	-0.763	-0.639	-0.686	28/04/23 (G0)	-0.523	-0.488	-0.130

Table 1 presents the correlation coefficients (r) between geomagnetic storm levels and TEC disturbances, as observed at two GNSS stations in Thailand: THBK station in Bangkok and THCP station in Chumphon. The TEC data are categorized into three sources GPS TEC, IGS TEC, and IRI TEC across multiple dates in March and April 2023. For the THBK station in Bangkok, the table shows both positive and negative correlations, varying according to storm intensity and date. Notably strong negative correlations occurred on March 23, 2023 (G2 storm), with coefficients of -0.825 (GPS TEC), -0.900 (IGS TEC), and -0.901 (IRI TEC), indicating a significant inverse relationship between geomagnetic storm intensity and TEC values on that day. In contrast, strong positive correlations were observed during March 24, 2023 (G4) and March 25, 2023 (G2), with the IRI TEC correlation peaking at 0.978 on 25 March. These results suggest that the impact of geomagnetic storms on TEC disturbances can vary significantly, even from one day to the next. Similarly, at the THCP station in Chumphon, high positive correlations are evident on April 23, 2023 (G1 storm), with coefficients of 0.544 (GPS TEC), 0.620 (IGS TEC), and 0.944 (IRI TEC), while strong negative correlations were found on April 22, 2023 (G0), particularly in the IRI TEC data (-0.894). The presence of both strong positive and negative values indicates complex interactions between geomagnetic activity and TEC behavior, which may differ between geographical locations and data sources. In general, the table highlights how the intensity of geomagnetic storms (ranging from G0 to G4) can influence TEC disturbances differently depending on the measurement method and location. This emphasizes the importance of analyzing multiple TEC data sources and stations to better understand the response of the ionosphere to space weather events.

IV. CONCLUSION AND DISCUSSION

In this study, the analysis of TEC behavior during severe geomagnetic storms (G4 level) in Solar Cycle 25 reveals a clear and measurable ionospheric response over low-latitude and near-equatorial regions. During storm occurrence periods, TEC values exhibit a noticeable increase followed by a gradual return to baseline levels within a few days. Specifically, TEC values increased by approximately 10–35% at the THBK station in Bangkok, located in the low-latitude region, and up to 75% at the THCP station in Chumphon, situated near the equatorial region. This demonstrates that geomagnetic storms significantly impact ionospheric TEC, particularly at lower latitudes where the equatorial ionization anomaly plays a crucial role. These findings align with previous studies. For instance, Chen et al. (2017, pp. 3632–3639) analyzed ionospheric TEC variations under both quiet and disturbed geomagnetic conditions using SWM and RMC methodologies. Their results showed an overestimation of disturbance occurrences by approximately 5–20% during storm periods, and up to 35% during quiet periods. In comparison, our study found TEC enhancements of more than 75% (THCP station) and 10-35% (THBK station) in near-equatorial regions highlighting the regional sensitivity to geomagnetic disturbances. Similarly, Jenan et al. (2021, pp. 575–587) investigated ionospheric TEC responses to the September 2017 geomagnetic storm and December 2019 annular solar eclipse over Sri Lanka. Their findings showed a TEC enhancement of approximately 11 TECU during the main phase of the storm, with the most significant variation observed at Kegalle. In contrast, our study found TEC values reaching up to 10-75 TECU on the storm day, further emphasizing the intense ionospheric impact in equatorial regions during G4-level storms.

With regard to the correlation analysis, the correlation coefficients (r) between geomagnetic storm levels and TEC disturbances demonstrate a significant and positive relationship. This indicates that the intensity of geomagnetic storms is strongly associated with TEC variability, particularly during G2-G4 level events. Higher storm levels tend to correspond with increased TEC values, reaffirming the sensitivity of the ionosphere to geomagnetic forcing in low-latitude and equatorial zones. Our results are also consistent with Nava et al. (2016, pp. 3421–3438), who studied ionospheric responses at mid- and low-latitudes. Their research reported an initial increase in TEC on storm days, followed by a subsequent decrease over several days, especially at mid-latitudes. However, at low latitudes, as similarly shown in our study, no post-storm reduction in TEC was observed, and enhancement patterns were more sustained.

In conclusion, the current study confirms that TEC variations are closely linked to geomagnetic storm intensity, with stronger storms yielding greater enhancements, especially in regions near the equator. This emphasizes the need for continuous monitoring of ionospheric behavior during space weather events to support GNSS-based applications in low-latitude countries like Thailand.

ACKNOWLEDGEMENT

We would like to thank the Institute of Geology and Geophysics, Chinese Academy of Sciences (IGGCAS), and the Earthquake Observation Division (EOD), Thai Meteorological Department (TMD) for supporting the BG2s GNSS receiver and sharing data. We would like to thank the International Reference Ionosphere (IRI) for IRI TEC and the International GNSS Service (IGS) for IGS TEC Maps for sharing data. We would like to thank the Space Weather Prediction Center (SWPC), and the National Oceanic and Atmosphere Administration (NOAA) organization for sharing data on geomagnetic storm activity. We would like to thank the World Data Center (WDC) for Geomagnetism, Kyoto, Japan, for sharing the AE and Dst indices data.

REFERENCES

Adolfs, M., Hoque, M. M., & Shprits, Y. Y. (2022). Storm-time relative total electron content modelling using machine learning techniques. *Remote Sensing, 14*(23), 1-17.

Ali, O. H., Zaourar, N., Fleury, R., & Amory-Mazaudier, C. (2021). Transient variations of vertical total electron content at low latitude during the period 2013–2017. *Advances in Space Research, 68*(12), 4857-4871.

Bilitza, D. (1990). *International Reference Ionosphere 1990 (Report no. NSSDC/WDC-A-R&S 90-22).* National Space Science Data Center *(*NSSDC) and World Data Center A for Rockets and Satellite (WDC-AR &S). https://ntrs.nasa.gov/api/citations/19910021307/downloads/19910021307.pdf.

Bilitza, D. (2001). International reference ionosphere 2000. *Radio Science, 36*(2), 261-275.

Bilitza, D., & Rawer, K. (1996). International Reference Ionosphere, in: W. Dieminger, G. Hartmann and R. Leitinger (Eds.), *The upper atmosphere - data analysis and interpretation* (pp. 735-772). Springer-Verlag.

Bilitza, D., & Reinisch, B. W. (2008). International Reference Ionosphere 2007: Improvements and new parameters. *Advances in Space Research, 42*(4), 599-609.

Blewitt, G. (1990). An automatic editing algorithm for GPS data. *Geophysical Research Letters, 17*(3), 199-202.

Bojilova, R., & Mukhtarov, P. (2023). Comparative analysis of global and regional ionospheric responses during two geomagnetic storms on 3 and 4 February 2022. *Remote Sensing, 15*(7), 1-23.

Brunini, C., Meza, A., Azpilicueta, F., Van Zele, M. A., Gende, M., & Díaz, A. (2004). A new ionosphere monitoring technology based on GPS. *Astrophysics and Space Science, 290*, 415-429.

Chen, Z., Wang, J. S., Deng, Y., & Huang, C. M. (2017). Extraction of the geomagnetic activity effect from TEC data: A comparison between the spectral whitening method and 28 day running median. *Journal of Geophysical Research: Space Physics, 122*(3), 3632-3639.

Chernyshov, A. A., Miloch, W. J., Jin, Y., & Zakharov, V. I. (2020). Relationship between TEC jumps and auroral substorm in the high-latitude ionosphere. *Scientific Reports, 10*(1), 1-13.

de Paula, E. R., de Oliveira, C. B., Caton, R. G., Negreti, P. M., Batista, I. S., Martinon, A. R., Neto, A. C., Abdu, M. A., Monico, J. F. G., Sousasantos, J., & Moraes, A. O. (2019). Ionospheric irregularity behavior during the September 6–10, 2017 magnetic storm over Brazilian equatorial–low latitudes. *Earth, Planets and Space, 71*(42), 1-15.

Dugassa, T., Habarulema, J. B., & Nigussie, M. (2019). Investigation of the relationship between the spatial gradient of Total Electron Content (TEC) between two nearby stations and the occurrence of ionospheric irregularities. In I. A. Daglis, C. Jacobi, & I. Mann (Eds.), *Annales Geophysicae* (Vol. 37, No. 6, pp. 1161-1180). Copernicus.

Goodwin, G. L., Silby, J. H., Lynn, K. J. W., Breed, A. M., & Essex, E. A. (1995). GPS satellite measurements: Ionospheric slab thickness and total electron content. *Journal of Atmospheric and Terrestrial Physics, 57*(14), 1723-1732.

Hofmann-Wellenhof, B., Lichtenegger, H., & Collins, J. (2012). Observables. In *Global positioning system: Theory and practice* (pp. 87-131). Springer-Verlag Wien GmbH.

Jenan, R., Dammalage, T. L., & Panda, S. K. (2021). Ionospheric total electron content response to September-2017 geomagnetic storm and December-2019 annular solar eclipse over Sri Lankan region. *Acta Astronautica, 180,* 575-587.

Kenpankho, P., Watthanasangmechai, K., Supnithi, P., Tsugawa, T., & Maruyama, T. (2011). Comparison of GPS TEC measurements with IRI TEC prediction at the equatorial latitude station, Chumphon, Thailand. *Earth, Planets and Space, 63*, 365-370.

Klimenko, M. V., Klimenko, V. V., Zakharenkova, I. E., Ratovsky, K. G., Korenkova, N. A., Yasyukevich, Y. V., Mylnikova, A. A., & Cherniak, I. V. (2017). Similarity and differences in morphology and mechanisms of the fo F2 and TEC disturbances during the geomagnetic storms on 26–30 September 2011. In *Annales Geophysicae* (Vol. 35, No. 4, pp. 923-938). Copernicus.

Kumar, K. V., Maurya, A. K., Kumar, S., & Singh, R. (2016). 22 July 2009 total solar eclipse induced gravity waves in ionosphere as inferred from GPS observations over EIA. *Advances in Space Research, 58*(9), 1755-1762.

Li, G., Ning, B., Zhao, X., Sun, W., Hu, L., Xie, H., Liu, K., & Ajith, K. K. (2019). Low latitude ionospheric TEC oscillations associated with periodic changes in IMF Bz polarity. *Geophysical Research Letters, 46*(16), 9379-9387.

Ma, G., & Maruyama, T. (2003, October). Derivation of TEC and estimation of instrumental biases from GEONET in Japan. In *Annales Geophysicae* (Vol. 21, No. 10, pp. 2083-2093). Copernicus.

Mansilla, G. A. (2019). Behavior of the Total electron content over the Arctic and Antarctic sectors during several intense geomagnetic storms. *Geodesy and Geodynamics, 10*(1), 26-36.

Mukaka, M. M. (2012). A guide to appropriate use of correlation coefficient in medical research. *Malawi Medical Journal, 24*(3), 69-71.

Nava, B., Rodríguez-Zuluaga, J., Alazo-Cuartas, K., Kashcheyev, A., Migoya-Orué, Y., Radicella, S. M., Radicella, C., Armory-Mazaudier, C., & Fleury, R. (2016). Middle-and low-latitude ionosphere response to 2015 St. Patrick's Day geomagnetic storm. *Journal of Geophysical Research: Space Physics, 121*(4), 3421-3438.

Nayak, C., Tsai, L. C., Su, S. Y., Galkin, I. A., Tan, A. T. K., Nofri, E., & Jamjareegulgarn, P. (2016). Peculiar features of the low-latitude and midlatitude ionospheric response to the St. Patrick's Day geomagnetic storm of 17 March 2015. *Journal of Geophysical Research: Space Physics, 121*(8), 7941-7960.

Pi, X., Mannucci, A. J., Lindqwister, U. J., & Ho, C. M. (1997). Monitoring of global ionospheric irregularities using the worldwide GPS network. *Geophysical Research Letters, 24*(18), 2283-2286.

Rao, S. S., Galav, P., Sharma, S., & Pandey, R. (2013). Low-latitude TEC variability studied from magnetically conjugate locations along 73° E longitude. *Journal of Atmospheric and Solar-Terrestrial Physics, 104*, 1-6.

Ratovsky, K. G., Klimenko, M. V., Dmitriev, A. V., & Medvedeva, I. V. (2022). Relation of extreme ionospheric events with geomagnetic and meteorological activity. *Atmosphere, 13*, 1-15.

Rawer, K., Bilitza, D., & Ramakrishnan, S. (1978a). Goals and status of the International Reference Ionosphere. *Reviews of Geophysics, 16*(2), 177-181.

Rawer, K., Bilitza, D., Ramakrishnan, S., & Sheikh, N. (1978b). Intentions and build-up of the International Reference Ionosphere. *Operational Modelling of the Aerospace Propagation Environment*, *1&2,* 6.1-6.10.

Reddy, C. A. (1986). The equatorial ionosphere. *Indian Journal of Radio & Space Physics, 15*(5&6), 247-263.

Reddybattula, K. D., Panda, S. K., Ansari, K., & Peddi, V. S. R. (2019). Analysis of ionospheric TEC from GPS, GIM and global ionosphere models during moderate, strong, and extreme geomagnetic storms over Indian region. *Acta Astronautica, 161*, 283-292.

Serafimov, K. B., Arshinkov, I. S., Bochev, A. Z., Petrunova, M. H., Stanev, G. A., & Chapkanov, S. K. (1982). A measuring equipment for electric and magnetic fields in the range of the ionosphere—Magnetosphere plasma mounted aboard the “Intercosmos-Bulgaria 1300” satellite. *Acta Astronautica, 9*(6-7), 397-399.

Skone, S., & de Jong, M. (2000). The impact of geomagnetic substorms on GPS receiver performance. *Earth, Planets and Space, 52*, 1067-1071.

Tsurutani, B. T., Lakhina, G. S., & Hajra, R. (2020). The physics of space weather/Solar-Terrestrial Physics (STP): what we know now and what the current and future challenges are. *Nonlinear Processes in Geophysics, 27*(1), 75-119.

Zhou, Y. L., Lühr, H., Xiong, C., & Pfaff, R. F. (2016). Ionospheric storm effects and equatorial plasma irregularities during the 17–18 March 2015 event. *Journal of Geophysical Research: Space Physics, 121*(9), 9146-9163.

1. Product of International Journal of Industrial Education and Technology (IJIET) called I-JIET. School of Industrial Education and Technology, King Mongkut's Institute of Technology Ladkrabang (KMITL) Submission Guideline

1. Printed schedule (Based on yearly calendar)

One issue per year as followings

- Issue 1 January – December

2. Scopes

Submission dateline: Continuing submission with no dateline.

Contemplation to publish journal article in Industrial education, and education and technology.

Journal article types: Original research articles, academic article, review article, and book review.

All articles have not been published or not been printed in any sources such as journal, conferences, so on.

3. **Who can submit**

- General publics who interest in the journal focusing fields.

4. Objectives

- For distributing on the research and academic issue industrial education and technology for all.
- For reporting the advantage and valuable issues on industrial education and technology.
- For exchanging the ideal and knowledge in industrial education and technology.

5. Publication

- Printed version is published as a promoted journal to associate on educational institution in public and private sector.
- Online version is published on database of TCI website https://ph02.tci-thaijo.org/index.php/IJIET/index

2. Main Research Paper Structure

Part 1 consists of

1.1 Title English should be shortly represented on the research goals

1.2 Authors Responded author and co-authors in English giving first name and last name but no title and referring by number.

1.3 ABSTRACT English should be shortly focused and directly scoped on the research objective, research methodology and the research summary. It should not exceed 250 - 300 words.

1.4 KEYWORDS English must choose keywords related to article.

Part 2 Contents

- **INTRODUCTION**

Including four paragraphs,

- First paragraph: Information based on articles in general.
- Second paragraph: Literature review on researches/articles related to the article in short
- Third paragraph: Selected researches/articles (from second paragraph)/methods specifically related to the article in short.
- Fourth paragraph: The objective of the article. Not writing in number of objectives.

- LITERATURE REVIEW

Including two paragraphs,

- First paragraph: Review of past and present researches/articles related to the article in more detail.
- Second paragraph: Research data/ Hypothesis for this article.

- RESEARCH METHODOLOGY

- Write about research methods and add picture, block diagram, and any graphics related to research methods.

- RESULTS (It should show the results in statistically significant according to objectives in table and or in graphic information).

- **CONCLUSION AND DISCUSSION**

Including two paragraphs,

- First paragraph: Conclude paragraph related to the results. Not writing in number of objectives.
- Second paragraph: Discuss the reasons of the results as it is or compare to other research's results. Not writing in number of objectives.

- **SUGGESTION** (If applicable) Not writing in number of objectives.

- **ACKNOWLEDGEMENT** (If applicable)

Do not give the credits to author/co-authors. No needs to put the number for this content and use the same size as the letter.

Part 3 References

- **REFERENCES**

The APA 7th edition reference style must be used as the requirement of International Journal of Industrial Education and Technology. The references are only referred to the research paper to be in this reference part. The writer is to be responsibility for the correction and the copyright of referring in the research.

3. Printed Format

3. Printed format

3.1 English Research Paper

Paper setting (6 - 10 pages (NOT exceed 11 pages))

- Font Th SarabunPSK only
- paper size top one inch bottom one inch left one inch right 0.8 inch

*Please follow the Template file which can be downloaded as .....

3.2 Titles

In English, using the Upper case (18 Bold inch)

3.3 Author and co-authors

It should be written in all righted authors. Identify the responded author with email. (15 Bold inch)

3.4 Abstract and contents

- Abstract is written in 14 bold inch and place it on the left side.
  The word “Abstract”, only letter A is upper case and others are 14 inches with one column.
- Contents are in one column with the headline in 16 bold inches and sub headline is in 14 bold inch. The contents are in 14 inches and given in five spaces.

3.5 Keywords: Fonts size 14 inches.

3.6 Figure and table

1. Leaving one row before inserting the table and giving one row before writing the information for the table in detail.
2. Uses “Table **...**” at the left corner with font 12 bold inch.
3. Table name is in font 12 inches and if the table detail is longer than one row, it should be started with new row by the same starting column.
4. Using only in column table as opened the left and right alignments.

Table 1: (Table name is in 12 inches.)

Title Z12 bold inch.	Title	Title	Title	Title
Content (12 inches.)	Content	Content	Content	Content
Content	Content	Content	Content	Content

Source: Kenpankho (2019)

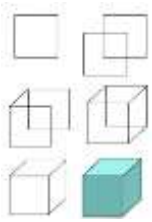

Figure 1: ..... (Font is in 13 inches with in center column)
Source: Kenpankho (2019, pp. 13-15)

3.7 Conclusion and Discussion in 16 inches.

On the left column for contents. For the first row in each paragraph, it must give four word-spaces (Font in 14 inches.)

3.8 Suggestion (If any) in 16 inches.

On the left column for contents. For the first row in each paragraph, it must give four word spaces (Font in 14 inches).

3.9 Acknowledgement (If any) in 16 inches. Without putting number in front of topic (Font in 14 inches).

No needs to put the number for this content (font in 14 inches).

3.10 References title font in 16 inches. (Content font is in 14 inches.)

3.11 $\bar{X}$ and table format

- Create your own table in column. Do not copy table form from other file sources.
- Use $\bar{X}$ as only in this following size $\bar{X}$ ($\bar{X} \geq 3.50$) ($\bar{X} = 4.51$).
- SD as Standard deviation.

3.12 Sub title format (Example)

I. Title (16 points)

A. Subtitle (Six word-spaces in 14 font inches.)

a. Second subtitle (alignment as the first world of subtitle in 14 font inches.)

1.1.1.1 Third subtitle

(1) Subtitle of 1.1.1.1

(1.1) Subtitle of (1)

4. Paper preparing/ Paper submitting for publishing in International Journal of Industrial Education and Technology Printed Format

For correction, perfection, and time saving, paper submission for publishing in International Journal of Industrial Education and Technology is needed to follow as this guideline.

1.1 Printed and typed in A4 paper size for 6-15 pages with one column style. By using Microsoft Word, it is highly recommended the word processing software that fits in the International Journal of Industrial Education and Technology format guideline according to our time saving for paper proof and publishing.

1.2 The original or submitted paper must be only formatted as the International Journal of Industrial Education and Technology printed format. **If the article does not follow directions, the author is informed, and the paper will not be stepped forward.**

1.3 Paper is needed to be clear in contents and pictures.

1.4 Paper has been not published or not printed in any sources such as journal, conferences, so on.

1.5 The corresponding author is fully responsibility to prove the correction of any requirement of International Journal of Industrial Education and Technology format.

1.6 Typing or writing journal application form.

1.7 Filling and signing on form to submit industrial education journal article. The first name is the author's name, then the second to sixth are co-authors' names and so on.

1.8 Preparing and submitting paper is noted as forms. URL at https://ph02.tci-thaijo.org/index.php/IJIET/index

1.8.1 Scan PDF file (.pdf) and Microsoft Word (.doc. or .docx.) to database and naming the files separately.

1.9 Competely fill out the member form of International Journal of Industrial Education and Technology. **Scan it, attach it to ThaiJo system, and post confirmed mail.**

1.10 Competely fill out the submitting form for International Journal of Industrial Education and Technology with requirement in 1.7.
Scan it, attach it to ThaiJo system, and post confirmed mail.

1.11 For the preparing and submitting paper, please see the direction and guideline of International Journal of Industrial Education and Technology as URL https://ph02.tci-thaijo.org/index.php/IJIET/index (Guideline is also in website).

Contact us

Mrs. Jantanee Supsaendee Assistant Editor
Mobile phone number 086 349 6020 (Office hours)
Telephone number 0 2329 8000 Exit 3720 (Office hours)
Fax number 0 2329 8435 (Office hours)

Address Academic Services for Social Affairs
(International Journal of Industrial Education and Technology, KMITL)
School of Industrial Education and Technology, King Mongkut's Institute of Technology Ladkrabang
No. 1, Soi Chalongkrung 1, Ladkrabang subdistrict, Ladkrabang district, Bangkok 10520 Thailand

If the author DOES NOT follow as the direction, paper will NOT BE considerred!

*****Link....Important needs*****

International Journal of Industrial Education and Technology (IJIET)

Website : https://ph02.tci-thaijo.org/index.php/IJIET/index

****Contact us if you have any questions****

E-mail : Journal.ided@kmitl.ac.th

IJIET

INTERNATIONAL JOURNAL OF INDUSTRIAL EDUCATION AND TECHNOLOGY

www.siet.kmitl.ac.th | www.tci-thaijo.org/index.php/IJIET
journal.ided@kmitl.ac.th 02 329 8000 ext. 3723
1 Chalongkrung Rd. Ladkrabang, Bangkok Thailand 10520